SELECTIVE CATALYTIC REDUCTION (SCR) OF NITRIC OXIDE WITH AMMONIA

USING Cu-ZSM-5 AND Va-BASED HONEYCOMB MONOLITH CATALYSTS:

EFFECT OF H_2 PRETREATMENT, NH_3-to-NO RATIO, O_2, AND SPACE VELOCITY

A Thesis

by

SAURABH GUPTA

Submitted to the Office of Graduate Studies of
Texas A&M University
in partial fulfillment of the requirements for the degree of

MASTER OF SCIENCE

August 2003

Major Subject: Mechanical Engineering

SELECTIVE CATALYTIC REDUCTION (SCR) OF NITRIC OXIDE WITH AMMONIA

USING Cu-ZSM-5 AND Va-BASED HONEYCOMB MONOLITH CATALYSTS:

EFFECT OF H$_2$ PRETREATMENT, NH$_3$-to-NO RATIO, O$_2$, AND SPACE VELOCITY

A Thesis

by

SAURABH GUPTA

Submitted to Texas A&M University
in partial fulfillment of the requirements
for the degree of

MASTER OF SCIENCE

Approved as to style and content by:

Jerald A. Caton	N. K. Anand
(Chair of Committee)	(Member)
D. F. Shantz	Dennis O'Neal
(Member)	(Head of Department)

August 2003

Major Subject: Mechanical Engineering

ABSTRACT

Selective Catalytic Reduction (SCR) of Nitric Oxide with Ammonia Using Cu-ZSM-5 and Va-Based Honeycomb Monolith Catalysts: Effect of H_2 Pretreatment, NH_3-to-NO Ratio, O_2, and Space Velocity. (August 2003)

Saurabh Gupta, B. Tech. (Hons.), Indian Institute of Technology

Chair of Advisory Committee: Dr. Jerald A. Caton

In this work, the steady-state performance of zeolite-based (Cu-ZSM-5) and vanadium-based honeycomb monolith catalysts was investigated in the selective catalytic reduction process (SCR) for NO removal using NH_3. The aim was to delineate the effect of various parameters including pretreatment of the catalyst sample with H_2, NH_3-to-NO ratio, inlet oxygen concentration, and space velocity.

The concentrations of the species (e.g. NO, NH_3, and others) were determined using a Fourier Transform Infrared (FTIR) spectrometer. The temperature was varied from ambient (25°C) to 500°C. The investigation showed that all of the above parameters (except pretreatment with H_2) significantly affected the peak NO reduction, the temperature at which peak NO reduction occurred, and residual ammonia left at higher temperatures (also known as 'NH$_3$ slip'). Depending upon the particular values of the parameters, a peak NO reduction of around 90% was obtained for both the catalysts. However, an accompanied generation of N_2O and NO_2 species was observed as well, being much higher for the vanadium-based catalyst than for the Cu-ZSM-5 catalyst. For both catalysts, the peak NO reduction decreased with an increase in space velocity, and did not change significantly with an increase in oxygen concentration. The temperatures at which peak NO reduction and complete NH_3 removal occurred increased with an increase in space velocity but decreased with an increase in oxygen concentration. The presence of more ammonia at the inlet (i.e. higher NH_3-to-NO ratio) improved the peak NO reduction but simultaneously resulted in an increase in residual ammonia. Pretreatment of the catalyst sample with H_2 (performed only for the Cu-ZSM-5 catalyst) did not produce any perceivable difference in any of the results for the conditions of these experiments.

DEDICATION

I would like to dedicate this thesis to my parents who have been a major influence in my life. They have supported me wholeheartedly in all my endeavors. I would also like to dedicate the thesis to my two sisters, who have been among my best friends and whose encouragement has kept me going throughout my student life.

ACKNOWLEDGEMENTS

TABLE OF CONTENTS

LIST OF FIGURES

LIST OF TABLES

1. INTRODUCTION

An important issue in atmospheric pollution control is the elimination of emissions of nitrogen oxides (NO_x) into the atmosphere. Nitrogen oxides emitted from mobile and stationary sources pose a substantial environmental hazard. NO_x in combination with other air pollutants such as SO_2 and volatile organic compounds contributes to acid rain, ground-level ozone, and photochemical smog [1].

Almost half of all anthropogenic NO_x emissions come from mobile sources, while the remainder comes from stationary ones, mainly combustion of fuels in power stations and industrial boilers [2]. Emissions of NO_x from motor vehicles are reduced by catalytic converters while several options are available for reducing emissions from stationary sources; both in-furnace and combustion control technologies are available. The unwanted air pollutants and the limited natural resources of fuels require an efficient control system for all combustion processes [3–4].

1.1 NO_x: A severe air pollutant

The term 'NO_x' usually refers to the two most common oxides of nitrogen; namely NO – nitric oxide and NO_2 – nitrogen dioxide. Among them, NO is of primary concern because of its high concentration relative to NO_2 in the exhaust. Though most nitrogen oxides are colorless and odorless, NO_2 is a reddish-brown gas with a sharp odor. It is the oxidation of NO to NO_2 that forms a part of the process that results in the creation of ozone in the lower level of the atmosphere [5]. Though ozone present in the upper-level of the atmosphere adsorbs the harmful ultraviolet rays from the sun, ground-level ozone causes human respiratory problem [6].

1.2 NO_x formation

NO_x formation mainly occurs through three mechanisms – Thermal NO_x, Fuel NO_x, and Prompt NO_x. In thermal NO_x process, reactions occurring at high temperatures during combustion processes generate both oxygen and nitrogen atoms by dissociation of respective molecules which subsequently lead to the formation of NO [7]. The quantity of NO_x formed depends on the reaction temperature, residence time, local stoichiometric composition and turbulence [8]. Three main reactions leading to the formation of thermal NO are described by the *Zeldovich* mecha-

---

This thesis follows the format and style of Journal of Fluids Engineering.

nism as below:

$$O + N_2 \Leftrightarrow N + NO \tag{1}$$

$$N + O_2 \Leftrightarrow O + NO \tag{2}$$

$$N + OH \Leftrightarrow H + NO \tag{3}$$
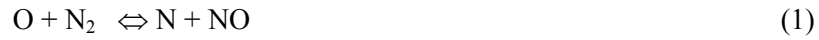
Although the rate of formation of thermal NO_x is slow in comparison to the other processes, it is the largest contributor to the total NO_x formed [9].

In fuel NO_x process, reaction occurs with fuel bound nitrogen at relatively low temperatures [10]. Between 20 and 80 percent of the bound nitrogen is typically converted to NO_x depending on fuel pyrolysis and subsequent reaction between many intermediate nitrogenous species and the oxidant species.

In prompt NO_x process, chemical reactions in thin oxygen-poor flame layers of premixed combustion produce HC radicals which form cyanides together with nitrogen that ultimately forms NO_x [11].

1.3 Methods of NO_x control

Methods of NO_x control can be categorized as pre- and post-combustion methods. In applications involving internal combustion engines, NO_x control is achieved by modification of the compression ratio, equivalence ratio, EGR (Exhaust Gas Recirculation), etc. These methods try to keep the combustion temperature low and are classified as pre-combustion techniques. The amount of NO_x reduction achieved through these methods is extremely limited and is insufficient for compliance with the stringent regulations. Post-combustion methods (also known as after-treatment methods) are more effective in this regard and are, therefore, relatively more popular [12]. Post-combustion techniques include Selective Catalytic Reduction (SCR), Selective Non-Catalytic Reduction (SNCR), etc.

1.4 Selective Catalytic Reduction (SCR) of NO_x

The Selective Catalytic Reduction (SCR) process uses a catalyst along with a reducing agent, usually NH_3, for the removal of NO_x. This is unlike a Selective Non-Catalytic Reduction (SNCR) process where only the reducing agent is used. The two techniques, Selective Catalytic Reduction and Selective Non-Catalytic Reduction, are compared in Table 1 [13].

Table 1. Comparison of SCR and SNCR techniques [13].

Features	SCR	SNCR
NO_x removal efficiency (%)	70 – 90	30 – 80
Operating temperature (°C)	200 – 500	800 – 1100
NH_3/NO molar ratio	0.4 – 1.0	0.8 – 2.5
NH_3 slip (ppm)	< 5	5 – 20
Capital cost	High	Low
Operating cost	Moderate	Moderate

From Table 1, it can be concluded that in comparison with SNCR, the SCR process has the advantage of higher NO_x removal efficiency at relatively lower operating temperatures. The disadvantage with using the SCR technique is the high capital cost in comparison with SNCR. Though an SCR system is generally designed to reduce NO_x emissions by 70–90%, higher reductions are possible. In an SCR process, several different catalysts e.g. metal-supported zeolites, mono-crystal and mixed phase catalysts, etc. operating over varying temperature windows can be used. In this work, primary focus will be on zeolites and vanadium-based catalysts. Suppliers provide catalyst samples in the form of powder, pellet, honeycomb monolith, etc. Most catalyst samples, after their usage, can be disposed off in a landfill or, in some cases, recycled.

The reaction of NH_3 with NO_x occurs within the catalytic bed at appropriate temperature conditions (200–400°C) in SCR process. The dominant reactions involving NH_3 and NO_x species are [14]:

$$4NO + 4NH_3 + O_2 \rightarrow 4N_2 + 6H_2O \tag{4}$$
$$6NO_2 + 8NH_3 \rightarrow 7N_2 + 12H_2O \tag{5}$$
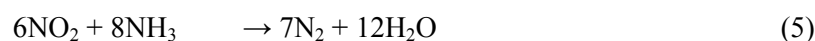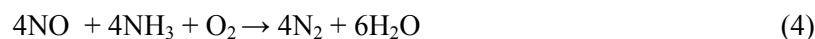
Ammonia gets chemisorbed on the active surface sites of the catalyst, where it reacts with the NO_x from the gas phase to yield molecular nitrogen and water vapor.

Some of the potential problems with the SCR system can be [13]:

(a) Emission of unreacted NH_3 (also known as 'NH_3 slip') which may give rise to complaints due to odor and potential health effects. In an SCR process, the NH_3 slip is generally <5

ppm, and levels lower than this are achievable which are far too low to pose any significant environmental hazard.

  (b) Emission of N_2O at high temperatures due to NH_3 oxidation:

$$2NH_3 + 2O_2 \rightarrow N_2O + 3H_2O \hspace{4cm} (6)$$

Recently, concern has been expressed about the potential contribution of N_2O to the greenhouse effect and global warming [13]. However, N_2O is not considered a serious pollutant from a public health point of view and its emission can be reduced by careful temperature control.

  (c) Catalyst poisoning from the deposition of sulfur and other compounds.

1.5 Zeolites

  Zeolites are one of the most well known inorganic molecular sieves [15]. The word 'zeolite' comes from the roots *zeo* (for boil) and *lithos* (for stone) in Greek. Water molecules in the zeolite pores are readily lost when the zeolites are heated. The word was coined by Cronstedt, a Swedish mineralogist, who observed a mineral which gave off steam and appeared to boil when heated [16].

  Zeolites are a well-defined class of crystalline naturally occurring aluminosilicate minerals. They have a three-dimensional structure arising from a framework of $[SiO_4]^{4-}$ and $[AlO_4]^{5-}$ coordination polyhedra linked by all their corners [17]. The frameworks are generally very open and contain channels and cavities in which cations and molecules are located, both of which have enough freedom of movement to permit cation exchange and reversible dehydration. Water molecules are located in these channels and cavities, as are the cations that neutralize the negatively charged framework.

  Many different zeolite structures exist, but the one which will be discussed in the present study is ZSM-5 (Zeolite Socony Mobil-5) [18]. ZSM-5 is a high silica zeolite with Si:Al ratio usually greater than 10. The present study focuses on the Cu-exchanged form of the ZSM-5 because this combination shows some of the highest known activities for the SCR of NO. Cu-ZSM-5 has the advantage of being able to reduce NO both with and without the addition of a reducing agent. Further experimental details on the SCR of NO using Cu-ZSM-5 catalyst are described in the literature review section.

1.6 Vanadium-based catalysts

Vanadium oxide may be deposited onto the surface of a wide variety of supports (including alumina, silica, zirconia, and titania) [19]. Such supported vanadium oxide materials find numerous applications, including their use as catalysts for the selective reduction reactions. Several studies in the past have investigated the structure and properties of supported vanadia. Of particular interest to the present study is their application to the selective catalytic reduction of NO. Supported vanadia catalysts show a high degree of effectiveness in selectively reducing NO in the presence of ammonia [20].

Further experimental details on the SCR of NO using vanadia-based catalysts are described in the literature review section.

2. LITERATURE REVIEW

In this section, previous experimental work done on the selective catalytic reduction process using ammonia as the reducing agent on the two catalysts: zeolite-based (Cu-ZSM-5) catalyst and vanadium-based (V_2O_5) catalyst will be presented.

2.1 Cu-ZSM-5 zeolite catalyst

Zeolites are crystalline alumino-silicates with tetrahedrally coordinated Al and Si elements. Since aluminum is trivalent, each aluminum tetrahedron is associated with a negative charge compensated by a counter-cation. This extended array creates an electrostatic field inside the zeolite. An ion pair could be stabilized within this field. The high activity of copper ion-exchanged ZSM-5 could be attributed to a preferred Cu site stabilized by ZSM-5 [21].

Copper is one of the most promising elements exchanged into zeolites that has the ability to activate nitric oxide for the reduction with ammonia or hydrocarbons and also for the decomposition into nitrogen and oxygen under lean-burn conditions [22]. To verify that it is indeed copper that is responsible for NO reduction, experiments were performed on H-ZSM-5 i.e. the base zeolite without copper-exchange. The results from these experiments were then compared with those performed on Cu-ZSM-5 catalyst under similar conditions. The two results are comp-

(a)   (b)
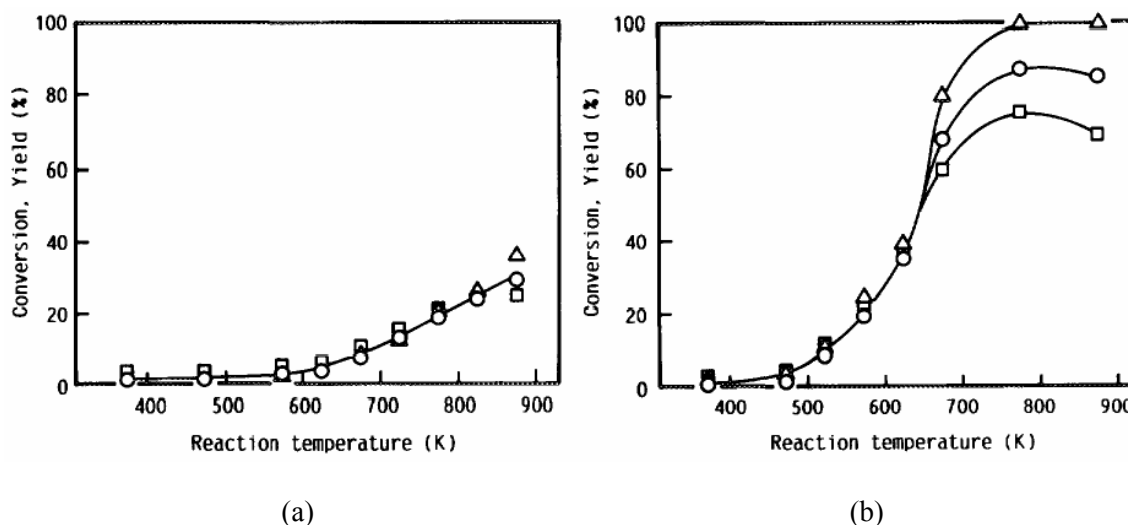
Figure 1. Reduction of nitric oxide with ammonia in the presence of O_2 on (a) H-Z(45) and (b) Cu(79)-Z(45). Conversion of NO ($\square$) and NH_3 (Δ), and yield of N_2 (o) were measured at W/F = 3.3 X 10^{-6} gm.hr/cm^3. Concentrations of reactants were 0.10% (both NO and NH_3) and 2% (O_2) in He carrier [22].

ared in Figure 1. The conversion of NO for H-ZSM-5 is much lower than that obtained for the Cu-ZSM-5 which confirms the role played by Cu^{2+}-ions exchanged into ZSM-5 in the reduction of NO. A significant increase in the conversion of NH_3 and yield of N_2 is also obtained for the Cu-ZSM-5 catalyst. Both the catalysts used were in the form of grains of 20–28 size mesh. In the experiments it was noted that the activity and the selectivity of the catalysts did not change for more than 48 hours of process time. The reaction products containing N-atom were N_2, NO_2 and N_2O. The amounts of N_2O and NO_2 formed were negligibly small for both the catalysts. For the ZSM-5 zeolite, it was also observed that the activity and selectivity of the catalyst varied with the extent of Cu^{2+}-exchange level and the Si/Al ratio of the ZSM-5.

A possible reaction scheme for the selective catalytic reduction of NO on Cu-ZSM-5 catalyst is shown in Figure 2 [22]. The active dimer species (a) has NH_3 ligands on each Cu^{2+} and one bridging oxygen and is located on two adjacent cation sites of the zeolite. A molecule of NO and dissociated oxygen react with the bridging oxygen, which results in the formation of bridg-
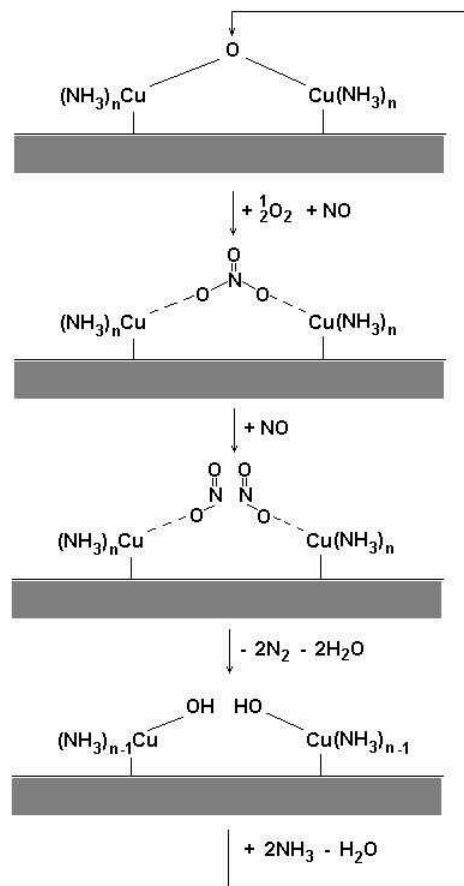
Figure 2. Reaction scheme of the SCR of NO with NH_3 in the presence of O_2 on Cu-ZSM-5 [22] (Redrawn).

ing NO_3 species (b). This step is considered the rate-determining step in the entire reaction scheme. Another molecule of NO attacks the NO_3 species to form two NO_2, one on each copper (c). The reactive NO_2 and one of the NH_3 ligands bound to the same Cu-ion react to produce N_2 and H_2O leaving an OH group and a coordinatively unsaturated site on each Cu (d). NH_3 can readily occupy the coordinatively unsaturated site, while dehydration from the two OH groups regenerates the initial dimer species (a). In this way, the entire reaction scheme could be repeated again.

Several parameters affect the extent of NO reduction in the selective catalytic reduction process using ammonia as the reducing agent. In the present work, we discuss the effect of four pertinent parameters: O_2 concentration, space velocity, concentration of the reducing agent, and pre-treatment with H_2.

2.1.1 Effect of O_2 concentration

The concentration of oxygen in the exhaust gas stream has a significant effect on the extent of NO conversion over Cu-ZSM-5 catalysts. In the complete absence of oxygen, typical NO conversions are usually low unless the temperature is raised above 1000 K. The introduction of even a slight amount of oxygen usually increases the NO conversion significantly at comparably lower temperatures [23]. However, the presence of oxygen beyond a certain limit (usually much beyond stoichiometric) again brings the NO conversion back to a lower value. This nature
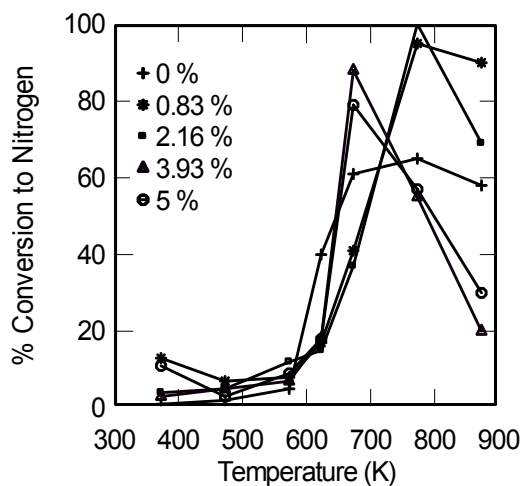
Figure 3. % NO conversion to N_2 over 1.8% Cu-ZSM-5 at various temperatures with different % O_2 in the reactant stream. Reactant stream contained 0.6% NO, 0.6% C_2H_4, variable O_2 and balance He flow totaling 30 ml per minute. 25mg of the catalyst used in this flow corresponded to a nominal GHSV of 36000 hr^{-1} [23] (Re-plotted).

of the effect of variation of oxygen concentration is plotted against temperature in Figure 3 for a Cu-ZSM-5 catalyst in powder form. In this particular case, a hydrocarbon, C_2H_4, has been used as the reducing agent. Under the conditions listed, high NO conversions were obtained when the O_2 concentration was typically around 1–2%. An almost complete conversion of NO to N_2 is obtained at 2.16% oxygen at a temperature of 773 K. O_2 concentrations considerably less than or higher than the typical value yielded lower NO conversions over the entire temperature range.

An excess of oxygen concentration reduces the catalyst selectivity towards N_2 formation and favors the formation of N_2O or even the oxidation of ammonia to NO or NO_2.

2.1.2 Effect of space velocity

Space velocity is defined as the volume ratio of gas flow rate relative to the catalyst volume, expressed in per-hour. At a constant gas flow rate, space velocity is inversely proportional to catalyst volume such that decreasing catalyst volume corresponds to increasing space velocity.

At low space velocities, copper exchanged zeolite catalyst, Cu-ZSM-5, shows high activity for sustained NO decomposition than most other catalysts. At high space velocities, typical of lean-burn engine exhaust, hydrocarbons aid in the selective reduction of NO over Cu-ZSM-5 [24]. In general, hydrocarbons display a certain degree of selectivity towards promoting NO reduction versus their reaction with O_2 in the presence of excess oxygen. The effect of space velocity on NO and hydrocarbon (C_3H_6) conversion is shown in Figure 4 for a Cu-ZSM-5 honeycomb monolith catalyst. The honeycomb monolith had a cell density of 400 square-channels per
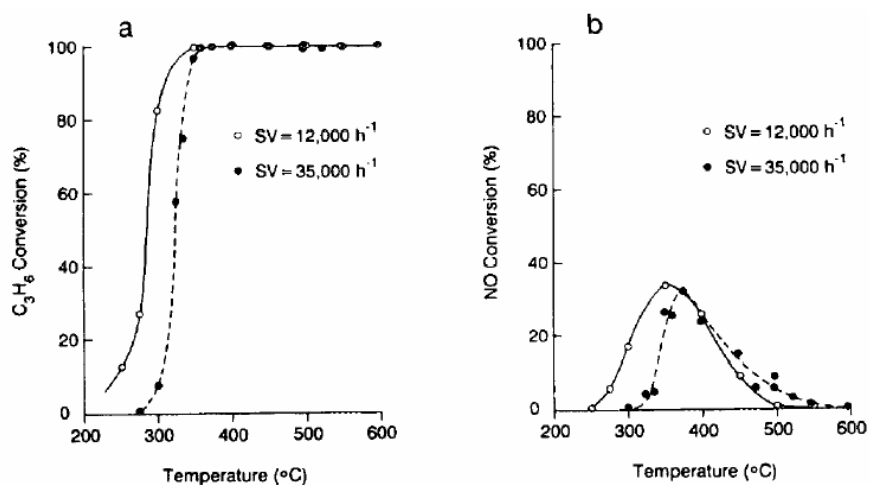
Figure 4. Effect of space velocity on the conversion of (a) C_3H_6 and (b) NO with varying temperature over Cu-ZSM-5 monolith. Reactant stream contained 230 ppm NO, 800 ppm C_3H_6, 7% O_2, and balance He [24].

sq. inch. As per the results, the light-off temperatures for both NO and HC conversion increase with the increase in space velocity. Interestingly, however, this shift of the conversion curve is much smaller for the decreasing portion of the NO conversion curve above the temperature of maximum NO conversion than for the increasing portion below it. A decrease in the peak NO conversion is also obtained as the space velocity is increased. It is worth noting that in spite of using as much as 800 ppm of C_3H_6 as against only 230 ppm of NO, full C_3H_6 conversion is achieved at the higher space velocity. This could be attributed to the presence of excess oxygen in the reaction.

2.1.3 Effect of reducing agent concentration

The concentration of the reducing agent with respect to NO or the NH_3-to-NO ratio affects the degree of NO_x reduction as well as the residual NH_3 concentration in a selective catalytic reduction process. Typically ammonia concentration can vary from a few ppm to several thousand ppm in the exhaust and hence, its variation significantly affects NH_3 conversion [25]. The effect of ammonia concentration for Fe(58)-ZSM-5(10) powder catalyst is shown in Figure 5. As the ammonia concentration decreases, the conversion of NH_3 increases significantly at the
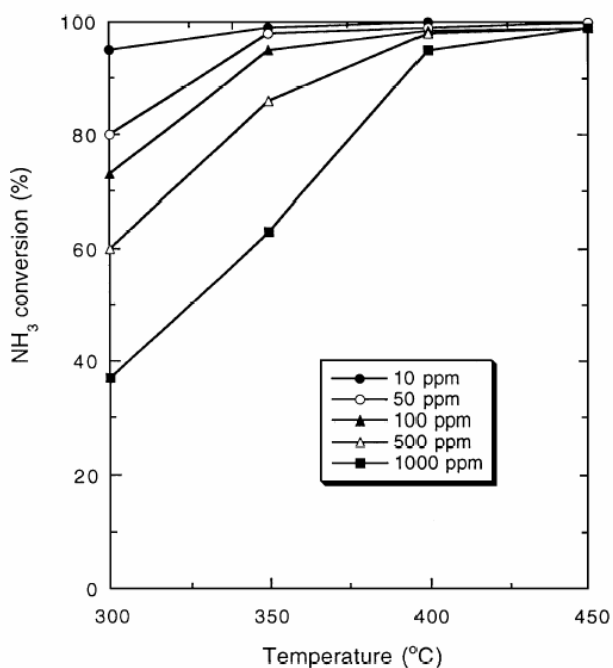
Figure 5. Effect of NH_3 concentration over Fe(58% exchange)-ZSM-5 (Si/Al = 10). Reaction conditions: 0.1gm of catalyst, [NH_3] = 10-1000 ppm, [O_2] = 2%, He = balance, total flow rate = 500 ml/min, and GHSV = 2.3 x 10^5 hr^{-1} [25].

lower temperatures. As shown in the figure, the ammonia conversion reached 95% at 300–450°C when the inlet ammonia concentration was only 10 ppm. It is worth noting that since the NH_3 concentration is plotted in percentage, a similar value does not mean an equal residual concentration in ppm. The 500 ppm NH_3 case in the figure would have a residual concentration as much as 5 times that of the 100 ppm case, though the plotted percentage values are the same.

2.1.4 Effect of pretreatment with hydrogen

Pretreatment refers to the step of exposing the catalyst to a single gas (in the current work, the gas being hydrogen) prior to flowing NO gas. Exposure to hydrogen is usually done at a particular temperature around 300°C and for a certain duration of time e.g. 1 hour.

Pretreatment of the Cu-ZSM-5 catalyst sample can be done in both oxidizing as well as reducing atmospheres. To expose the catalyst sample to reducing atmospheres, CO or H_2 gas is flown over it, whereas oxygen is used in the case of oxidizing atmospheres. Based on the catalyst sample, pretreatment affects the degree of NO reduction. In the case of Cu-ZSM-5, the degree of copper exchange on the ZSM-5 determines the affect of pretreatment on NO reduction [26]. Under-exchanged Cu-ZSM-5 zeolites i.e. those with copper exchange <100% (by weight) do not seem to be affected by pretreatment of hydrogen at 150°C for 30 minutes at a flow rate of 30 ml per min. However, for over-exchanged Cu-ZSM-5, a reduction in peak NO conversion is obtained for the same pretreatment.

2.2 Vanadium-based catalyst

Vanadium oxide (V_2O_5) is a popular base oxide catalyst for the selective catalytic reduction of NO_x with ammonia. Bosch and Janssen [27] tested several base oxide catalysts e.g. V_2O_5, Fe_2O_3, CuO, NiO, etc. for the selective catalytic reduction of NO with ammonia and found vanadium oxide to be the most active and selective catalyst among them. The deposition of vanadium oxide as well as other oxides on supports leads to an increase in their catalytic activity. The nature of the support is a very important factor and TiO_2-SiO_2 support shows among the best activity [28]. The structure of vanadia supported over titania catalysts is shown in Figure 6.
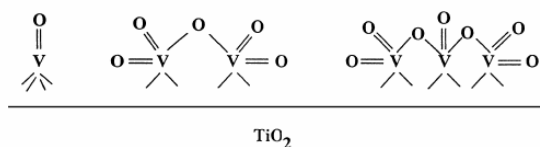
Figure 6. Structural forms of vanadia-supported titania catalysts [28].

Figure 7 shows the conversion of NO and NH_3 on vanadia-titania catalysts with different vanadia contents [28]. It can be observed that an optimum V_2O_5 loading is necessary for higher NO conversions. V_2O_5 loading different than this value leads to lower NO conversions. As per the figure, V_2O_5 loading in the range of 1–20% yields the best results. This however, cannot be said about NH_3 conversions. Higher V_2O_5 loading seems to favor higher NH_3 conversion.
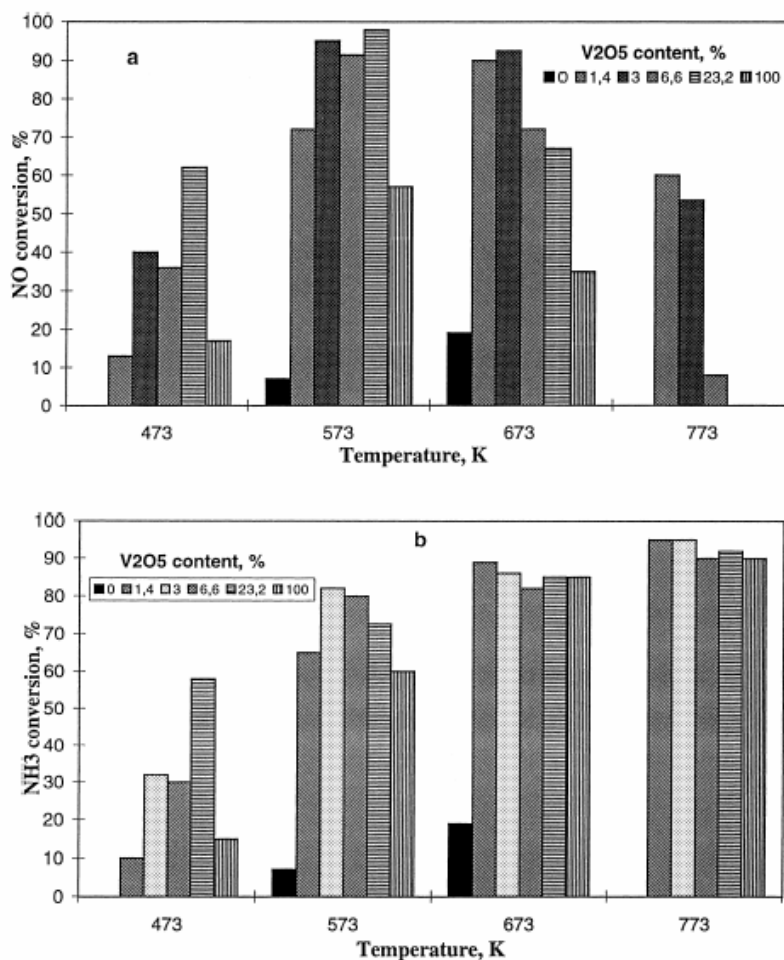
Figure 7. NO (a) and NH_3 (b) conversions on vanadia-titania catalysts with different content of vanadia (50 mg catalyst, NH_3-to-NO ratio = 1.38, O_2 = 3500 ppm) [28].

Similar to the analysis done for Cu-ZSM-5 catalyst, the next section examines the effect of different parameters over NO reduction and NH_3 conversion using vanadium-oxide catalyst supported on cordierite ceramic honeycomb.

2.2.1 Effect of O_2 concentration

In the case of vanadium-oxide catalyst supported on cordierite ceramic honeycomb, inlet oxygen content only has a slight affect on the NO reduction. This nature is as shown in Figure 8 [29]. A high NO conversion is obtained when the oxygen content is in the range of 5–7%, which is similar to the emission of industrial flue gas.
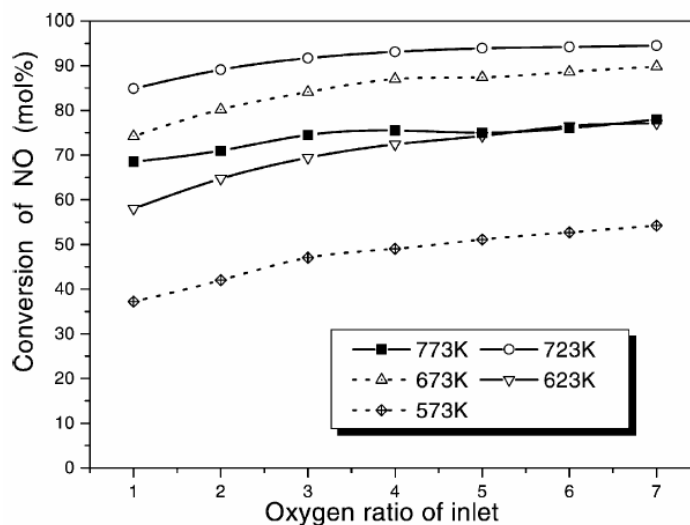
Figure 8. The correlation between inlet oxygen concentration and NO conversion at various temperatures on V_2O_5-MoO_3-WO_3/TiO_2/Al_2O_3/cordierite-honeycomb (SV = 6000 hr^{-1}, NH_3 = 1000 ppm, NO = 1000 ppm, variable O_2, balance N_2) [29].

2.2.2 Effect of space velocity

Typically, an increase in the space velocity decreases the NO conversion for most catalysts since the net residence time of the gas species over the surface of the catalyst decreases [29]. To some extent, temperature plays a role in determining the degree to which space velocity affects the NO conversion. As shown in Figure 9, an increase in space velocity results in a decrease in the NO conversion at temperatures higher than 573 K. The situation shown in the figure for 573 K appears, however, to be an anomaly. Since for this particular temperature, an increase of NO conversion is observed with an increase in space velocity.
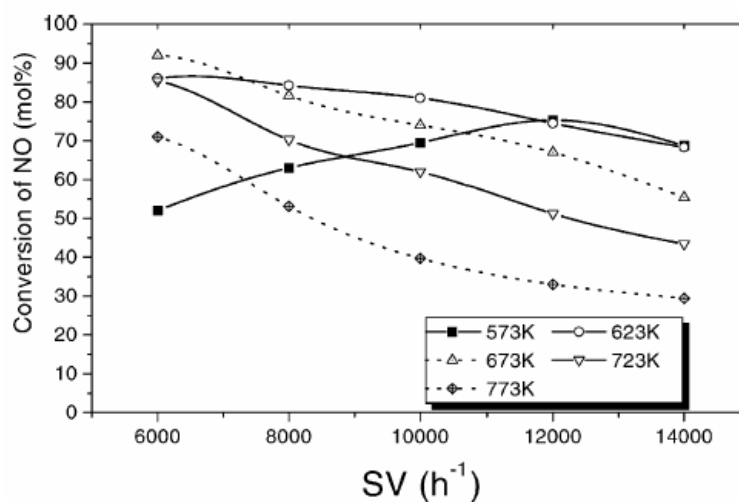
Figure 9. The correlation between space velocity and NO conversion at various temperatures on V_2O_5-MoO_3-WO_3/TiO_2/Al_2O_3/cordierite-honeycomb (O_2 = 5%, NH_3 = 1000 ppm, NO = 1000 ppm, balance N_2) [29].

2.2.3 Effect of reducing agent concentration

Figure 10 shows the effect of inlet NH_3-to-NO ratio over the conversion of NO at various temperatures [29]. NH_3-to-NO ratio does not have a very significant effect on the NO conversion, though a slightly higher NO conversion is obtained at higher NH_3-to-NO ratios.
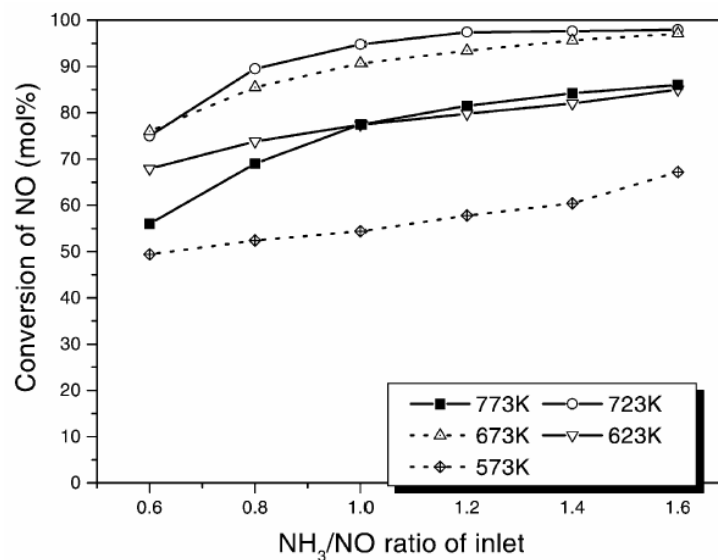
Figure 10. Correlation between NH_3/NO ratio and NO conversion at various temperatures on V_2O_5-MoO_3-WO_3/TiO_2/Al_2O_3/cordierite-honeycomb (O_2 = 5%, SV = 6000 h^{-1}) [29].

Any variation in NO conversion is not observed when NH_3-to-NO ratio is in the range of 1.2–1.6. Therefore, one can conclude that NH_3-to-NO ratio of 1.2 is high enough for getting a reasonable NO conversion.

3. OBJECTIVES

The overall goal of this research project is to experimentally investigate the selective catalytic reduction (SCR) of NO_x by ammonia using zeolite-based (Cu-ZSM-5) and vanadium-based catalysts. In the first part of this work, the effect of different parameters e.g. pretreatment with hydrogen, NH_3-to-NO feed ratio, inlet oxygen concentration, and space velocity over Cu-ZSM-5 zeolite-based catalyst will be investigated. In the second part, the effect of all the above-mentioned parameters, except pretreatment with hydrogen, under similar conditions will be investigated over vanadium-based catalyst. The two sets of results will then be compared with each other.

4. EXPERIMENTAL APPARATUS

The experimental apparatus consists of four distinct systems: (1) source of simulated exhaust gas, (2) mass flow controllers, (3) the furnace and reactor assembly with the catalyst sample (reaction zone), and (4) the output gas mixture analysis system (Fourier transform infrared spectrometer). Each of these systems is described in detail in the following sections.

4.1 Overview of the experimental system

The experimental apparatus is shown in Figure 11. First, the mass flow controllers were calibrated individually with various gases (NO, O_2, NH_3, H_2, and N_2) and had accuracies $\pm 1.0\%$ of full scale. The mixture of gases entered the reactor inside the furnace. The total flow rate of the gas was 1100 sccm (standard cubic centimeter per minute at 0°C and 1 atm). A quartz tube (ID=10 mm, length=1.04 m) was placed in a three-zone reactor that has an electronic control unit to furnish accurate temperature control. The cylindrical-shaped catalyst sample was placed inside the quartz-tube, towards the middle of the tube along the length. The output gas from the reactor was diluted by 5000 sccm of nitrogen gas and then passed through a 60 micron-filter. The output gases from the reactor, including the dilution gas, flowed into the gas cell of the FTIR spectrometer. Necessary calibrations were completed to quantify the FTIR spectrum for each species, prior to the main experiments. Then, the gases were vented out to the atmosphere.

4.2 Source of simulated exhaust gas

To avoid the inherent complexities of dealing with the exhaust from an actual combustion source, such as particulate emissions and transient irregularities in NO concentrations, a source of simulated exhaust gas was used. All the gases and gas mixtures were stored in standard gas cylinders. The concentration of each cylinder is listed in Table 2.
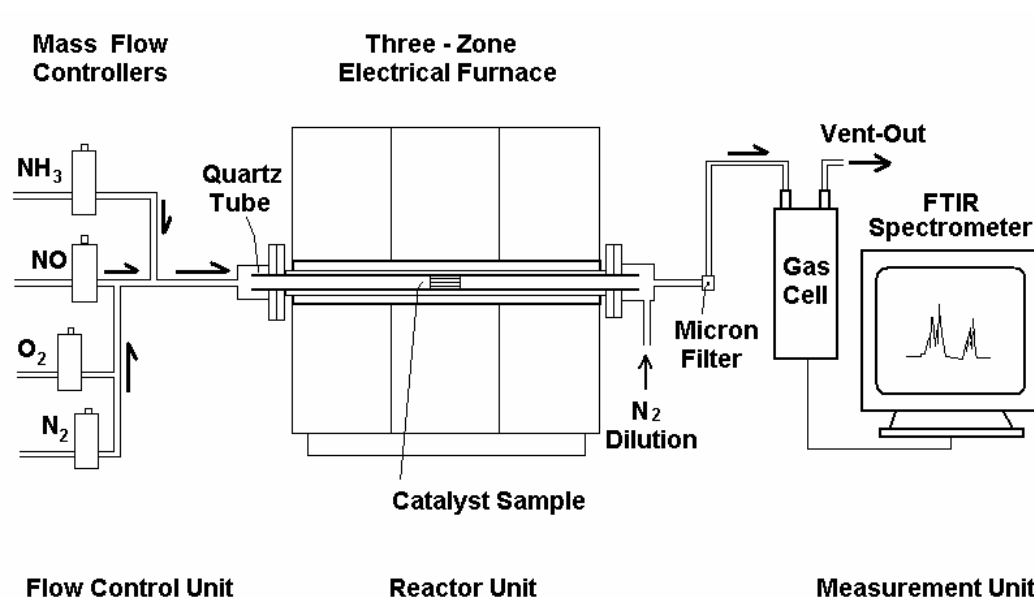
Figure 11. Schematic of the experimental system.

Table 2. Cylinder concentrations used for the experiments.

Species	Mixture	Purity
N_2	100 % N_2	99.99%
O_2	48.91% O_2, 51.09% N_2	± 1%
NO	1.04% NO, 98.96% N_2	± 1%
NH_3	0.5207% NH_3, 99.4793% N_2	± 1%
H_2	5.1% H_2, 94.9% N_2	± 1%

4.3 Mass flow controller

As a means of controlling the flow of each constituent gas into the system, a series of six mass flow controllers were used (the PFD 401 series by Precision Flow Devices Inc., and MKS type 1179A by MKS Instruments). Table 3 lists the manufacturer details of all the controllers, their flow capacity and the gases.

Table 3. Mass flow controllers in the experimental system.

MFC-Number	Manufacturer	Flow capacity (sccm)	Gas used
1-2	MKS Instruments	100	O_2/N_2
1-3	MKS Instruments	200	NO/N_2
1-4	MKS Instruments	5000	N_2
2-1	Precision Flow Devices	300	NH_3/N_2
2-2	Precision Flow Devices	300	O_2/N_2
2-4	Precision Flow Devices	1000	N_2 or H_2/N_2

4.3.1 Calibration process

The gas that flows through the system was collected in a glass flask. This flask was initially completely filled with water, which gets displaced by the gas over time [30]. The time and volume displaced are measured, and the time rate of change of the volume was found through the following equation [31]:

$$\frac{\partial V}{\partial t} = \frac{M_1 - M_2}{\rho_{H2O} * t} \tag{7}$$

To include the pressure difference from changing water level in the flask during the process of displacement, a correction term for the volume is needed [30]:

$$\frac{\partial V_{adjusted}}{\partial t} = \left(\frac{P_{atm} - \rho_{H2O}gh}{P_{atm}} \right) \left(\frac{M_1 - M_2}{\rho_{H2O}t} \right) \tag{8}$$

The procedure is described in more detail in Appendix 1.

4.4 Catalyst sample, furnace and reactor assembly (reaction zone)

The experiments were performed on two catalyst samples: zeolite-based (Cu-ZSM-5) and vanadium-based catalysts. Further details about the two samples are as listed in Appendix 2. Figure 12 shows the photographs taken of the two catalyst samples.

(a)   (b)
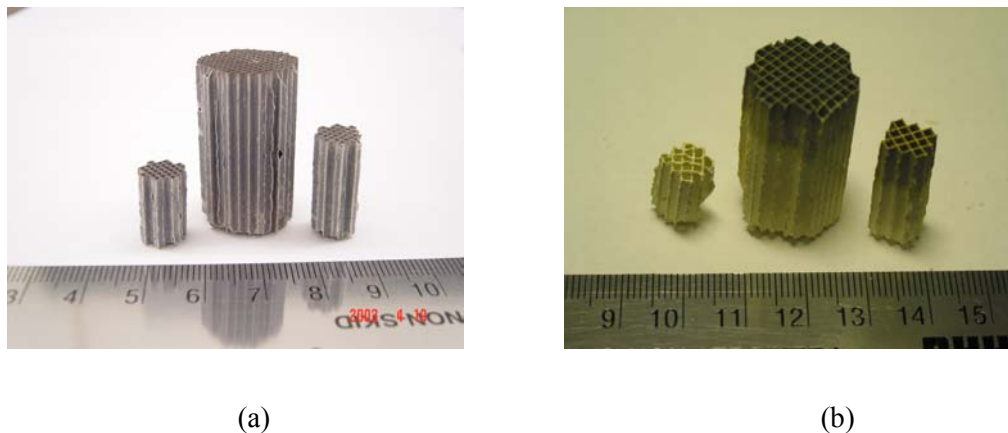
Figure 12. Samples of (a) Cu-ZSM-5, and (b) Va-based catalysts.

The catalyst sample procured from the supplier had to cut to desired size for obtaining a particular space velocity.

Space velocity is defined as the volume ratio of gas flow rate relative to the catalyst volume, expressed in per-hour. At a constant gas flow rate, space velocity is inversely proportional to catalyst volume such that decreasing catalyst volume corresponds to increasing space velocity. Table 4 lists the three space velocity values at which the two samples were tested. The total flow rate of the gas mixture through the tube was 1100 sccm (standard cubic centimeter per minute at 0°C and 1 atm).

Careful cutting of the sample was also desired to make a snug fit into the quartz-tube, aimed at minimizing the 'slip' of gases past the catalyst surface. Figure 13 shows a honeycomb sample put into a cylindrical tube.

Table 4. Space velocity calculation.

Tube radius [r] (cm)	Catalyst sample length [l] (cm)	Volume of catalyst [$V (= \pi r^2 l)$] (cm^3)	Space velocity $SV' = 1100 / V$ (min^{-1})	Space velocity $SV = SV'$ x 60 (hr^{-1})
1	3	9.425	116.7	7000
0.5	2	1.571	700.3	42000
0.5	1.3	1.021	1077.4	64000

The mixture of gases flowing through the reactor were heated to desired temperatures by a three-zone tube furnace (Lindberg model number 54259), which has an electronic control unit (Lindberg model number 58475). The initial and final zones of the furnace are 15.2 cm in length while the center zone is 30.5 cm in length as shown in Figure 14. The energy produced by the heating zones is transferred to an Inconel 600 pipe in the entire length of the furnace. The quartz
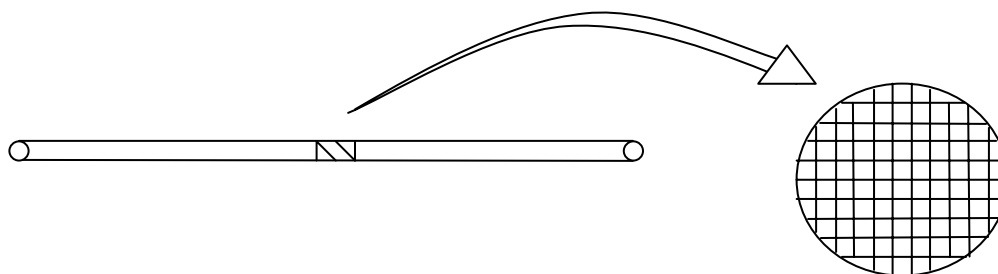
Figure 13. Schematic of honeycomb catalyst sample put inside cylindrical quartz tube.

reactor, which prevents catalytic reactions with the steel surface, is centrally located within this pipe. The reactor contains 25.4 mm internal diameter tube of Inconel 600 which is 1.06 m in length. The tube is threaded at both ends and two 6.35 mm bolt flanges of 304 stainless steel are screwed on the ends. The quartz tube is located in the center of the reactor with the support of graphite gaskets made from Grafoil^{TM} sheets. These gaskets also seal the flanges on each end of reactor. The furnace temperature distribution is described in more detail in Appendix 3. The catalyst sample was put somewhere along the center of the tube, along the length; corresponding to the middle of Zone-2.
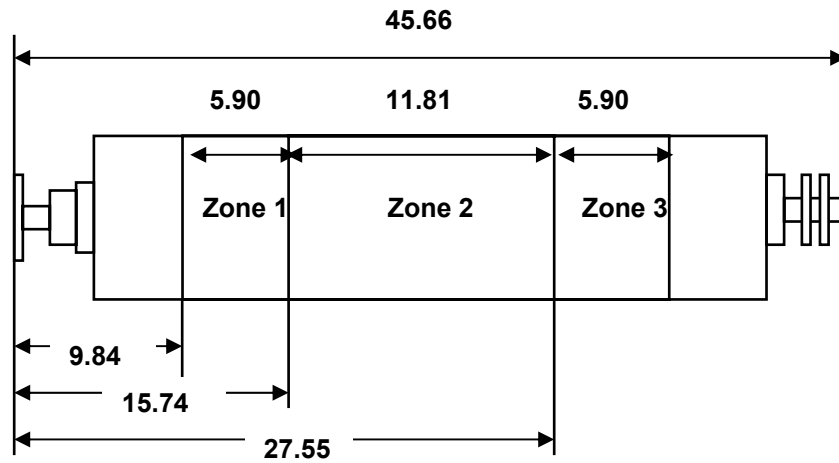
Figure 14. Schematic of the furnace system. All lengths in inches [30].

4.5 The output gas mixture analysis system (Fourier Transform Infrared Spectrometer).

In order to determine the concentration of the various species exiting the reactor, a Fourier transform infrared (FTIR) spectrometer was used (Bio-Rad FTS-60A). After dilution the total simulated exhaust stream of 6100 sccm passed through a permanently aligned long path cell. A liquid nitrogen cooled MCT (Mercury-Cadmium-Tellurium) detector which works in the range of 4000 to 400 cm^{-1} was used.

To operate the FTIR properly, the FTS 60A uses cold water and liquid nitrogen as coolants. Besides, since the beam splitter is made out of KBr crystal, which is sensitive to ambient air conditions, a purge air generator was used to ensure proper air conditions.

The calibration procedure of the different species used in the experiments for FTIR is consistent with that followed by Park [32].

5. EXPERIMENTAL PROCEDURE AND OBSERVATIONS

The total flow rate of the gases passing through the reactor was 1100 sccm (standard cubic centimeter per minute at 0°C and 1 atm), regulated by the mass flow controllers. This standard condition is consistent with former studies completed by Park [32].

5.1 Procedure for conducting experiments

First, liquid nitrogen, used as a coolant, was added to the MCT detector. The mass flow controllers need to be turned on at least sometime before the experiment begins. The whole system was tested for leakage before the experiment everyday. MFC #1-4 and #2-4, through which the nitrogen gas flows, were switched on first to take background scan with the FTIR.

The setting of each mass flow controller was determined using an Excel spreadsheet, which included the calibration data for each specific mass flow controller. The mass flow controller setting was double-checked to ensure the flow of the correct quantities of each mixture component. The furnace was turned on to ensure thermal stability. During the course of the experiments, the temperature of the furnace was increased by 50°C or 100°C, as per the requirement, from ambient to 500°C.

Upon taking the last reading at 500°C, the flow of all species except N_2 was stopped. The nitrogen gas flowed through the furnace (at 1100 sccm) till it cooled back to the ambient temperature, which normally took more than 3 hours with fan assistance. During the cooling process, the presence of some water was picked up by the FTIR.

Pretreatment of the catalyst sample was done by exposing the catalyst sample to only a particular gas (in our case, hydrogen using a 5% H_2 and balance N_2 mixture) at the flow rate of 1100 sccm. Pretreatment was completed prior to the beginning of the experiments. This step was performed for a time duration of 1 hour while keeping the reactor at a temperature of 300°C. At the end of the time period, the reactor was cooled back to the ambient temperature before starting the usual flow of NO, NH_3, and the other species.

5.2 Data collection procedure

To process the data of a FTIR scan, Bio-Rad WinIR-pro version 2.96 software was used. The scan of the gas mixture in the FTIR was taken after steady state was established, which

could be monitored by comparing scans of the FTIR repeatedly. That is to say, the final value was reached once the change of the measured concentration was within ± 0.5 ppm, which was assumed as a steady state. Typically, the final values for each reading were obtained in about 30 minutes. The furnace needed some time to reach the set temperature. The measured temperature was for the outside Inconel 600 steel tube.

An FTIR measurement was the average of 16 scans, which were reported as one data value. The calibration procedure of the different species used in the experiments for FTIR is consistent with that followed by Park [32]. All data were obtained from low to higher temperature in the reactor. The concentration data was then plotted as a function of temperature.

5.3 Observations

During the calibration step of the species (prior to running the main experiments), each reading normally took around 15–20 minutes to reach steady state. However, during the calibration of the NH_3 specie, each reading took up to 1 hour to stabilize.

Only Zones 2 and 3 of the furnace were used to heat the catalyst sample and pre-heat the incoming gas mixture, respectively, to the desired temperatures. However, an automatic increase in the temperature for Zone 1 was observed. With temperatures in Zones 2 and 3 set to 500°C, the temperature for Zone 1 rose up to around 200°C, by itself.

During the course of the experiments, every time the furnace temperature was increased, a sudden 'burst' of NH_3 concentration was observed. Though an NH_3 concentration of only 330 ppm was metered through the MFC, the FTIR measured value would rise above 1000 ppm, though temporarily. This was observed for every experiment, for a temperature increase by as low as 25°C, especially when initial temperatures were higher than 300°C.

For the experiments performed in the complete absence of O_2 specie, every reading took considerably large amounts of time, more than 2 hours each, to reach steady state.

6. EXPERIMENTAL RESULTS AND DISCUSSION

The results obtained for the selective catalytic reduction of NO with ammonia as the reducing agent using Cu-ZSM-5 and vanadium-based catalysts will be presented and discussed. As a preface to this section, lines in all figures used to connect data points are only for the purpose of helping the reader differentiate one set of data from another.

6.1 Using Cu-ZSM-5 zeolite-based catalyst

Table 5 summarizes the experimental cases performed using copper ion-exchanged ZSM-5 zeolite (Cu-ZSM-5) catalyst in the form of a honeycomb monolith. The listed cases cater to the variation of four parameters: inlet oxygen concentration, space velocity (SV), NH_3-to-NO ratio, and pretreatment with hydrogen.

6.1.1 Effect of O_2 concentration

Figures 15 and 16 show the effect of inlet oxygen concentration (the amount metered into the reactor along with other gas species, on a molar percentage basis) on the NO reduction and NH_3 conversion, respectively. The experimental conditions were: NO = NH_3 = 330 ppm, SV = 7000 hr^{-1}, without pretreatment with H_2. In the figures, NO reduction is defined as the ratio of output NO concentration (as measured by the FTIR) to the input NO concentration (as metered through the MFC), in percentage form. Similarly, the NH_3 conversion is defined as the ratio of output NH_3 concentration (as measured by the FTIR) to the input NH_3 concentration (as metered through the MFC), in percentage form.

As can be observed from Figure 15, the temperature at which peak NO reduction occurs successively decreases as the oxygen concentration is increased from 0 to 0.5%. However, no significant difference is observed if the oxygen concentration is increased further to 3%. Since the inlet NO and NH_3 concentrations are only 330 ppm, or 0.033%, an oxygen concentration of even 0.5% provides over a factor of 10 greater amount. The peak NO reduction seems to be unperturbed by any variation in oxygen concentration, barring the minor fluctuations due to the experimental uncertainty in measurement. This is a highly favorable result considering the recent drive towards lean-burn conditions, which entails a high oxidizing environment in the exhaust.

Table 5. Experimental cases performed on Cu-ZSM-5 honeycomb monolith catalyst.

NH$_3$ = 264 ppm	SV = 42000 hr^{-1}	O$_2$ = 0.1 %	Both with and without H$_2$ pretreatment
		O$_2$ = 0.5 %	Both with and without H$_2$ pretreatment
		O$_2$ = 3 %	Without H$_2$ pretreatment
NH$_3$ = 330 ppm	SV = 7000 hr^{-1}	O$_2$ = 0 %	Both with and without H$_2$ pretreatment
		O$_2$ = 0.1 %	
		O$_2$ = 0.5 %	
		O$_2$ = 3 %	
	SV = 42000 hr^{-1}	O$_2$ = 0 %	Both with and without H$_2$ pretreatment
		O$_2$ = 0.1 %	
		O$_2$ = 0.5 %	
		O$_2$ = 3 %	
	SV = 64000 hr^{-1}	O$_2$ = 0.1 %	Without H$_2$ pretreatment
		O$_2$ = 0.5 %	
		O$_2$ = 3 %	
NH$_3$ = 660 ppm	SV = 7000 hr^{-1}	O$_2$ = 0 %	Without H$_2$ pretreatment
		O$_2$ = 0.5 %	
		O$_2$ = 3 %	
	SV = 42000 hr^{-1}	O$_2$ = 0.1 %	Without H$_2$ pretreatment
		O$_2$ = 0.5 %	
		O$_2$ = 3 %	

Figure 16 shows the effect of variation of inlet oxygen concentration on NH$_3$ conversion. The lowest temperature at which complete NH$_3$ conversion occurs successively decreases upon increase of inlet oxygen concentration. The presence of extra oxygen facilitates the oxidation of ammonia at a lower temperature. No significant difference is observed, though, between oxygen concentrations of 0.5% and 3%. Note that in the complete absence of oxygen, even at 500°C only around 80% NH$_3$ conversion is achieved.

It remains to be seen what effect the variation of inlet NH$_3$-to-NO ratio, space velocity, and pretreatment with hydrogen bring about, if any.
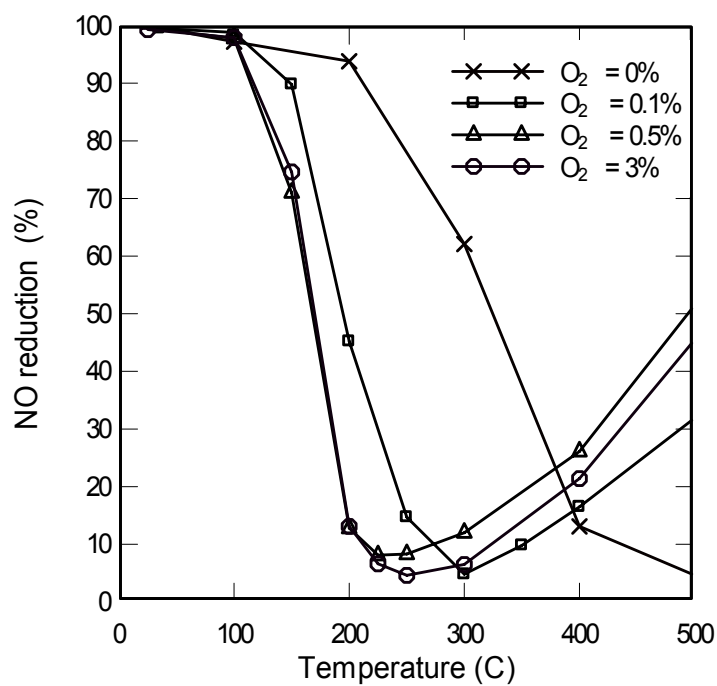
Figure 15. NO reduction at different oxygen concentrations using Cu-ZSM-5. The reaction conditions are: NO = NH$_3$ = 330 ppm, SV = 7000 hr^{-1}, without pretreatment with H$_2$.
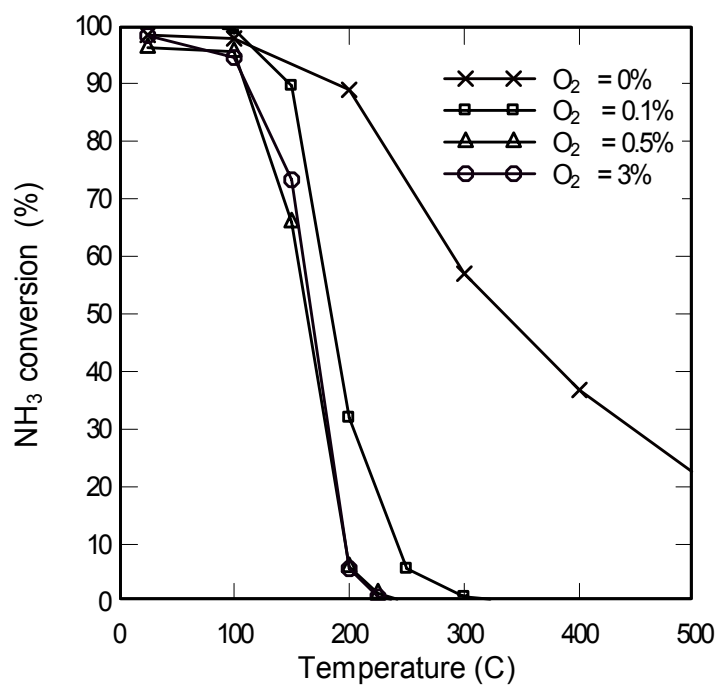
Figure 16. NH$_3$ conversion at different oxygen concentrations using Cu-ZSM-5. The reaction conditions are: NO = NH$_3$ = 330 ppm, SV = 7000 hr^{-1}, without pretreatment with H$_2$.

6.1.2 Effect of space velocity

Space Velocity (SV) is defined as the volume ratio of gas flow rate relative to the catalyst volume, expressed in hour^{-1}. At a constant gas flow rate, space velocity is inversely proportional to catalyst volume such that decreasing catalyst volume corresponds to increasing space velocity. As listed in Table 5, experiments were performed for three different space velocities. The values were suitably chosen to gauge the effect over a wide range of variation.

Figures 17 and 18, together with the previous two figures, show the effect of variation in
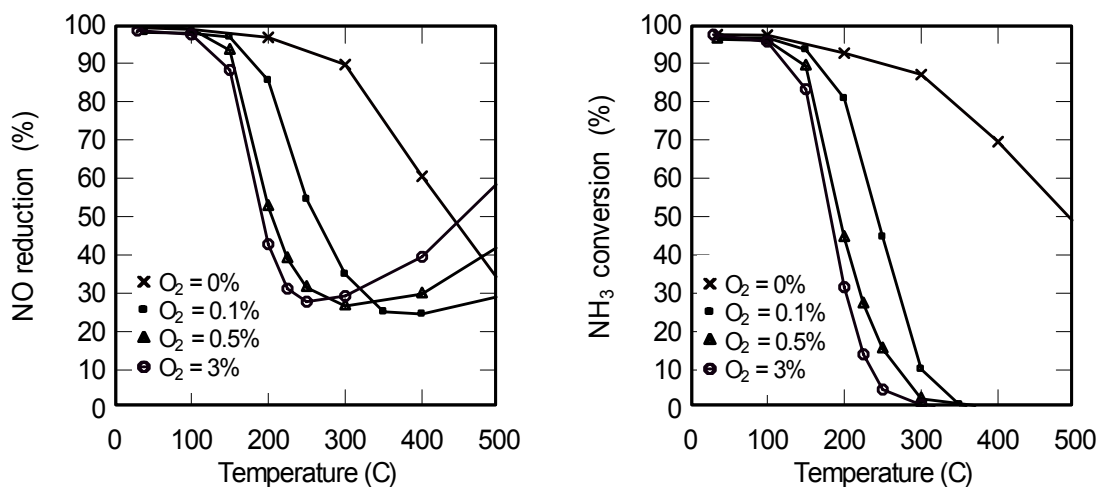
Figure 17. NO reduction and NH$_3$ conversion at different O$_2$ concentrations using Cu-ZSM-5. The reaction conditions are: NO = NH$_3$ = 330 ppm, SV = 42000 hr^{-1}, no pretreatment with H$_2$.
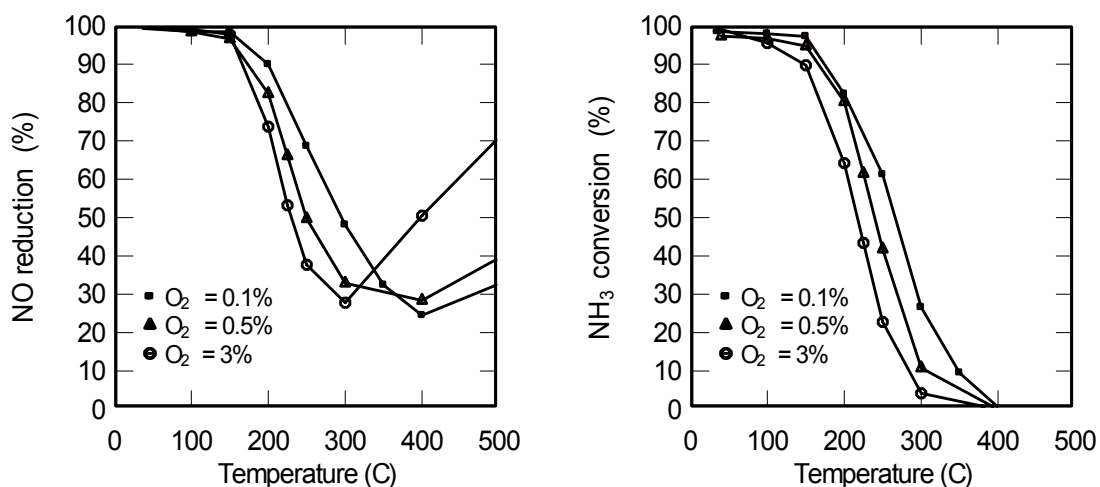
Figure 18. NO reduction and NH$_3$ conversion at different O$_2$ concentrations using Cu-ZSM-5. The reaction conditions are: NO = NH$_3$ = 330 ppm, SV = 64000 hr^{-1}, no pretreatment with H$_2$.

the space velocity on NO reduction and NH_3 conversion using a Cu-ZSM-5 catalyst. Though the peak NO reduction drops from around 95 to 75% when the space velocity is increased from 7000 to 42000 hr^{-1}, no marked change is observed upon further increasing it to 64000 hr^{-1}. This nature of the variation is shown separately in Figure 19. Note that the x-axis in the figure is a logarithmic scale.
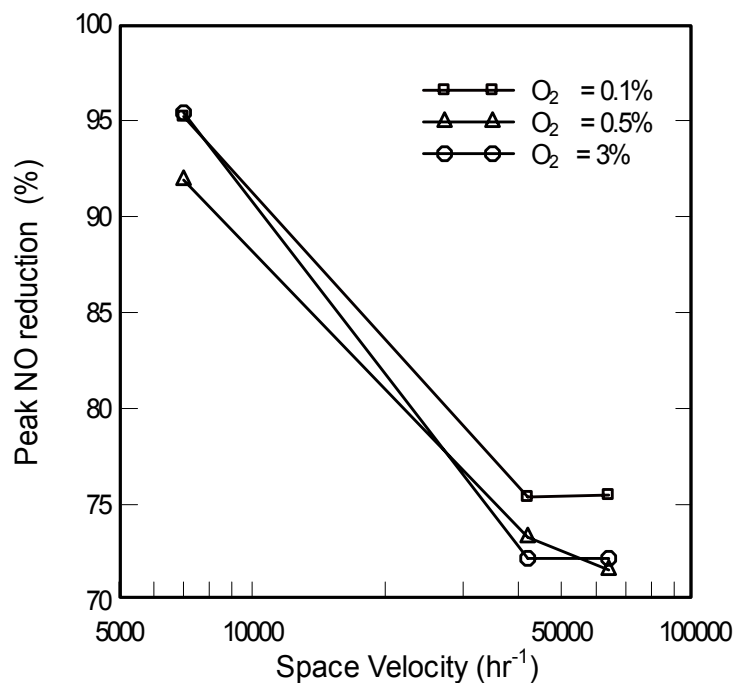
Figure 19. Variation in peak NO reduction with space velocity at different oxygen concentrations using Cu-ZSM-5. The reaction conditions are: NO = NH_3 = 330 ppm, without pretreatment with H_2.

Another approach towards analyzing the effect of space velocity on NO reduction is to find the variation in the total temperature range for which a high NO reduction is observed. This result is presented in Figure 20. The choice of a figure of 70% NO reduction is purely based on convenience. (As an example, for the case with O_2 = 0.1% and SV = 64000 hr^{-1} (Figure 18), NO reduction greater than 70% is observed between temperatures of 360°C and 470°C, giving a total temperature range of 110°C). As can be observed, the total temperature range for which NO reduction remains greater than 70% continuously decreases as the space velocity is increased.
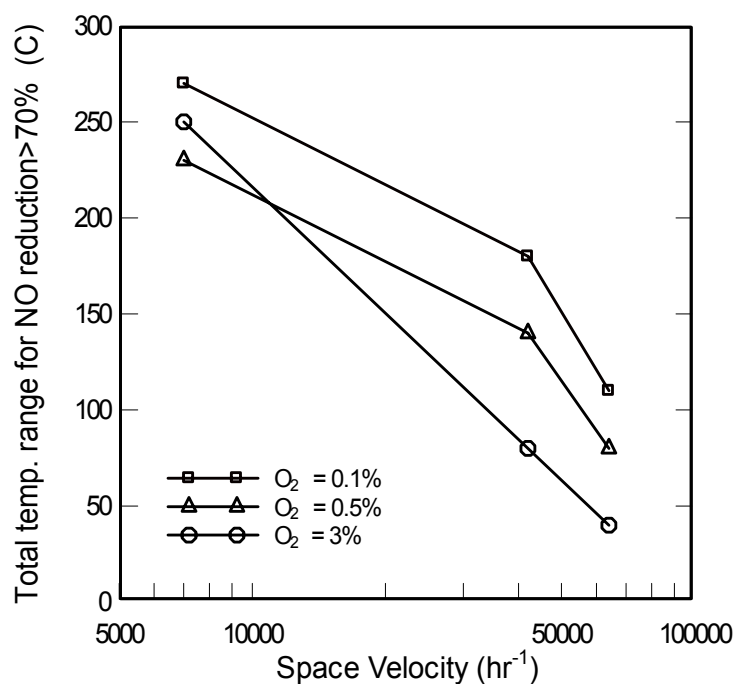
Figure 20. Variation in total temperature range for which NO reduction is greater than 70%, at different oxygen concentrations using Cu-ZSM-5. The reaction conditions are: NO = NH$_3$ = 330 ppm, without pretreatment with H$_2$.

Figure 21 shows the effect of space velocity on the lowest temperature at which complete NH$_3$ conversion is achieved. As the space velocity is increased, the lowest temperature at which complete NH$_3$ conversion occurs also successively increases. A higher oxygen concentration seems to favor complete NH$_3$ conversion at a lower temperature (irrespective of the space velocity), as the curve corresponding to 3% oxygen concentration lies below the other two curves corresponding to oxygen concentrations of 0.1% and 0.5%, respectively. Also, the curves corresponding to oxygen concentrations of 0.5% and 3% are closer together as compared to 0.1% and 0.5%, though the increase in oxygen concentration is higher for the former two than the latter. This indicates that an oxygen concentration of 0.5% is sufficiently lean to cause a significant difference in the lowest temperature at which complete NH$_3$ conversion is obtained.
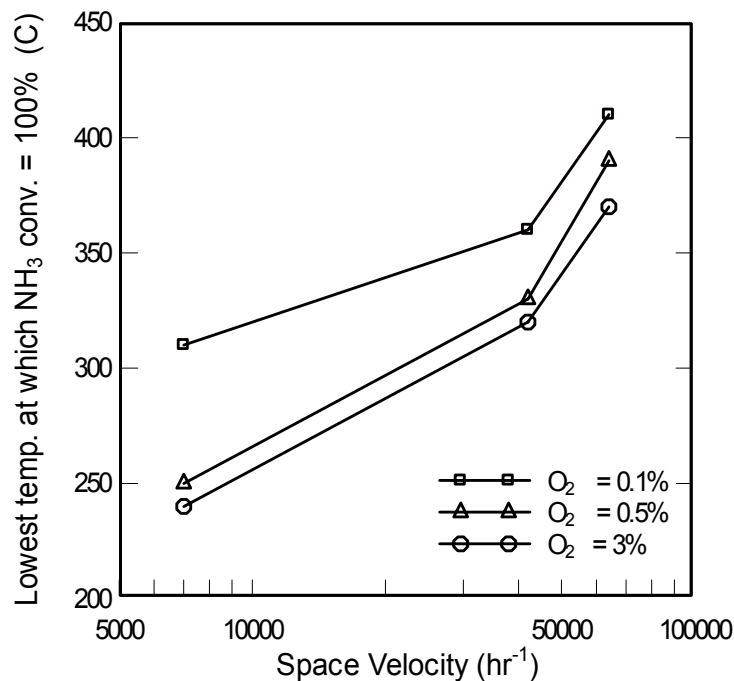
Figure 21. Variation in temperature at which NH_3 conversion is 100%, at different oxygen concentrations using Cu-ZSM-5. The reaction conditions are: NO = NH_3 = 330 ppm, without pretreatment with H_2.

6.1.3 Effect of ammonia concentration

The variation in the inlet ammonia concentration from 264 to 660 ppm, as also listed in Table 5, results in the variation of NH_3-to-NO ratio from 0.8 to 2.0, respectively. Figure 22 shows

Figure 22. NO reduction and NH_3 conversion at different O_2 concentrations using Cu-ZSM-5. The reaction conditions are: NO = 330 ppm, NH_3 = 660 ppm, SV = 7000 hr^{-1}, no pretreatment with H_2.

the effect of high ammonia concentration, corresponding to an NH_3-to-NO ratio of 2.0, for a space velocity of 7000 hr^{-1}. It can be compared with Figure 15 and 16 which show the NO reduction and NH_3 conversion, respectively, at the same space velocity, but at an NH_3-to-NO ratio of unity.

It can be observed that the presence of more ammonia increases the total temperature range at which higher NO reduction is obtained; which is highly desirable. In addition, in spite of the presence of a high concentration of ammonia, complete ammonia conversion is achieved by about 300°C (in the presence of some oxygen concentration).

Experiments on each of the three NH_3-to-NO ratios were performed at a space velocity of 42000 hr^{-1}, which is more typical of the exhaust from automotive sources. NO reduction and NH_3 conversion results for NH_3-to-NO ratio of unity, at a space velocity of 42000 hr^{-1}, were presented in Figure 17. Figures 23 and 24 show the results at the same space velocity for an NH_3-to-NO ratio value of 0.8 and 2.0, respectively. Note the variation in the peak NO reduction as the NH_3-to-NO ratio varies. Also note the variation in the temperature at which complete NH_3 conv-

Figure 23. NO reduction and NH_3 conversion at different oxygen concentrations using Cu-ZSM-5. The reaction conditions are: NO = 330 ppm, NH_3 = 264 ppm, NH_3-to-NO ratio = 0.8, SV = 42000 hr^{-1}, without pretreatment with H_2.

ersion is obtained with the variation in NH_3-to-NO ratio. These two results are quantified in Figures 25 and 26, respectively. Note that the results are plotted with the x-axis being a log-scale. As shown in Figure 25, peak NO reduction successively improves as the NH_3-to-NO ratio in-

creases from 0.8 to 2.0, though the variation in oxygen concentration does not produce a perceivable difference.
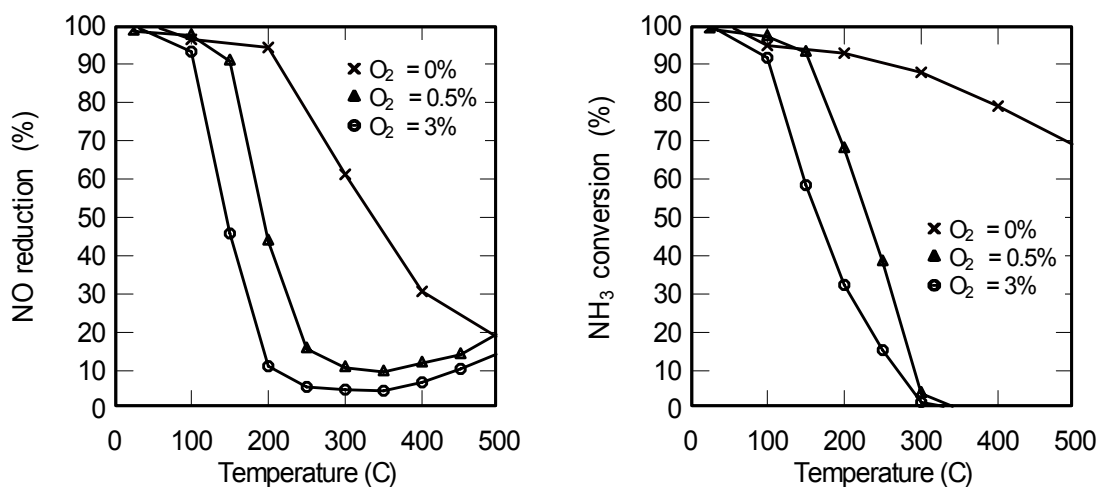

Figure 24. NO reduction and NH_3 conversion at different oxygen concentrations using Cu-ZSM-5. The reaction conditions are: NO = 330 ppm, NH_3 = 660 ppm, NH_3-to-NO ratio = 2.0, SV = 42000 hr^{-1}, without pretreatment with H_2.
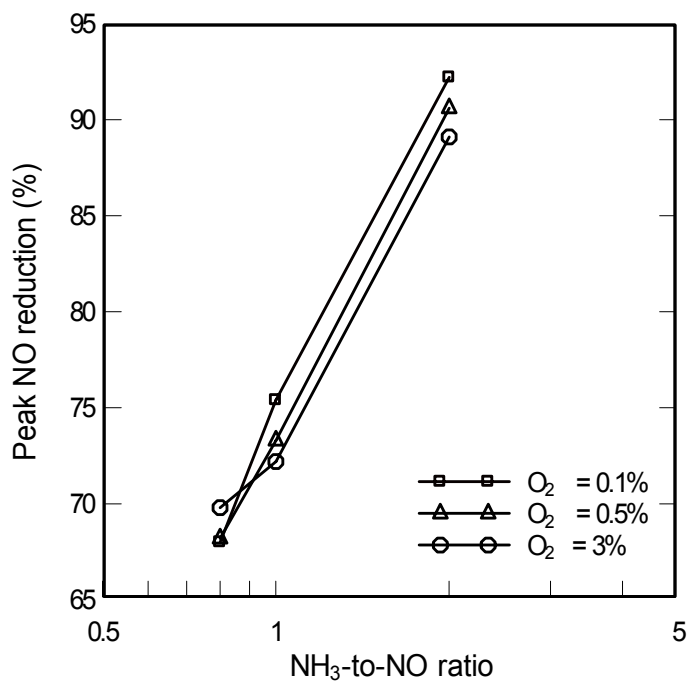
Figure 25. Variation in peak NO reduction with NH_3-to-NO ratio at different O_2 concentrations using Cu-ZSM-5. The reaction conditions are: SV = 42000 hr^{-1}, no H_2 pretreatment.
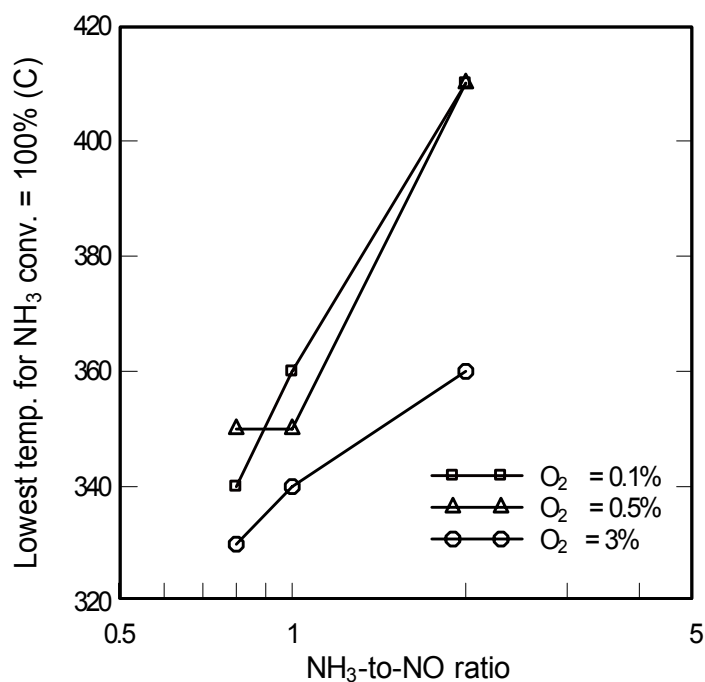
Figure 26. Variation in lowest temperature at which complete NH_3 conversion occurs with NH_3-to-NO ratio at different oxygen concentrations using Cu-ZSM-5. The reaction conditions are: $SV = 42000 \ hr^{-1}$, without pretreatment with H_2.

In Figure 26, the lowest temperature at which complete NH_3 conversion is obtained is plotted against NH_3-to-NO ratio. Upon observation, one can see the steady rise in the temperature for complete NH_3 conversion with an increase in NH_3-to-NO ratio. Therefore, though an increase in NH_3-to-NO ratio favors higher NO reduction, it is accompanied with the higher temperature requirement to completely eliminate ammonia from the exhaust.

Figure 27 shows the variation in temperature at which peak NO reduction is obtained with the variation in NH_3-to-NO ratio. A higher oxygen concentration seems to favor peak NO reduction at lower temperatures. At a particular oxygen concentration, the lowest temperature for peak NO reduction occurs at an NH_3-to-NO ratio of unity. This is true irrespective of the particular oxygen concentration.
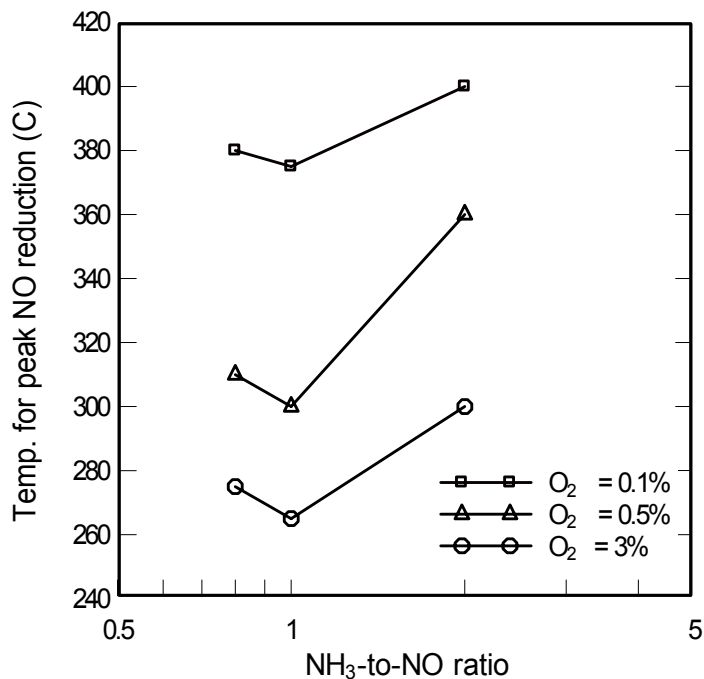
Figure 27. Variation in temperature for peak NO reduction with NH_3-to-NO ratio at different oxygen concentrations using Cu-ZSM-5. The reaction conditions are: SV = 42000 hr^{-1}, without pretreatment with H_2.

6.1.4 Effect of pretreatment with hydrogen

Pretreatment refers to the step of exposing the catalyst to a specific gas, in our case hydrogen, prior to flowing NO gas. Exposure to hydrogen is usually done at a particular temperat-
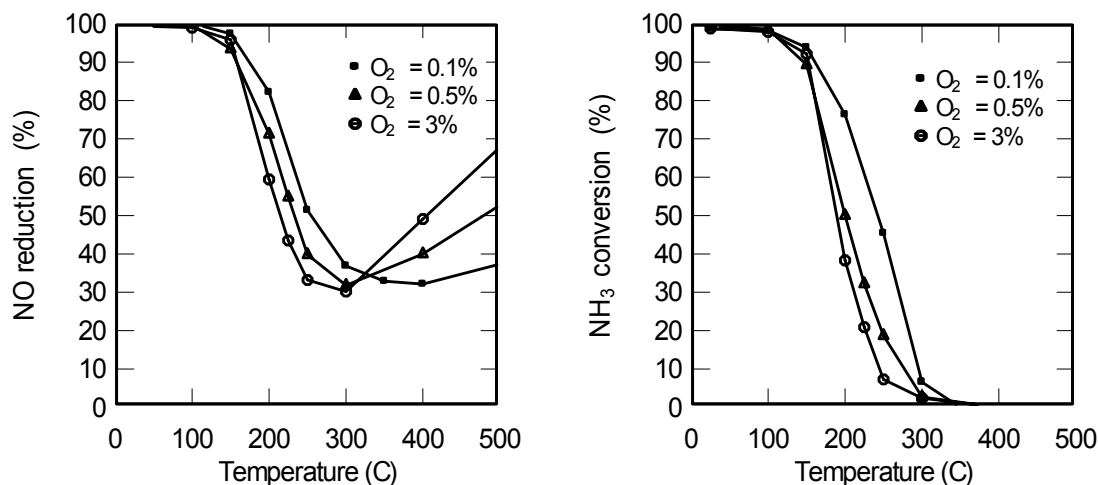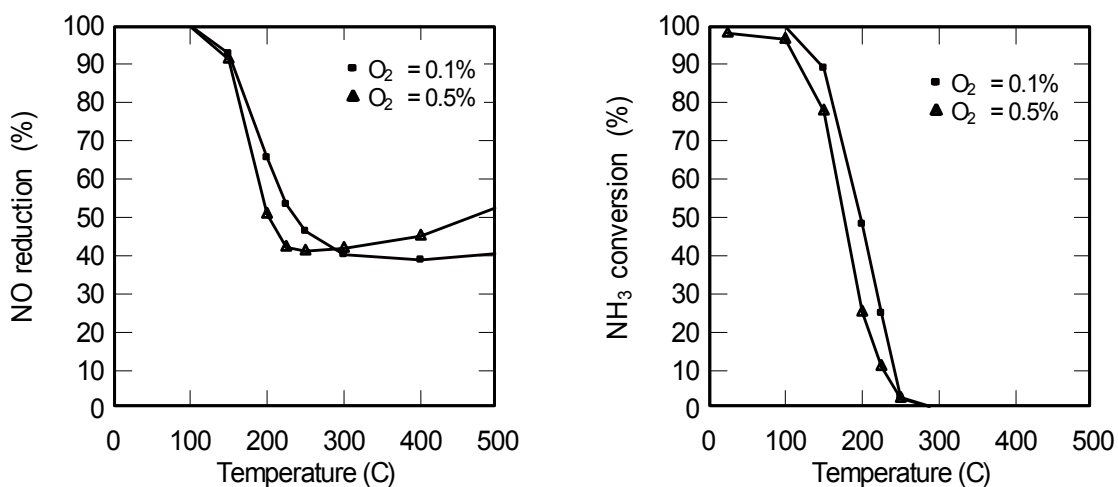

Figure 28. NO reduction and NH_3 conversion at different oxygen concentrations using Cu-ZSM-5. The reaction conditions are: NO = 330 ppm, NH_3 = 264 ppm, NH_3-to-NO ratio = 0.8, SV = 42000 hr^{-1}, with pretreatment with H_2.
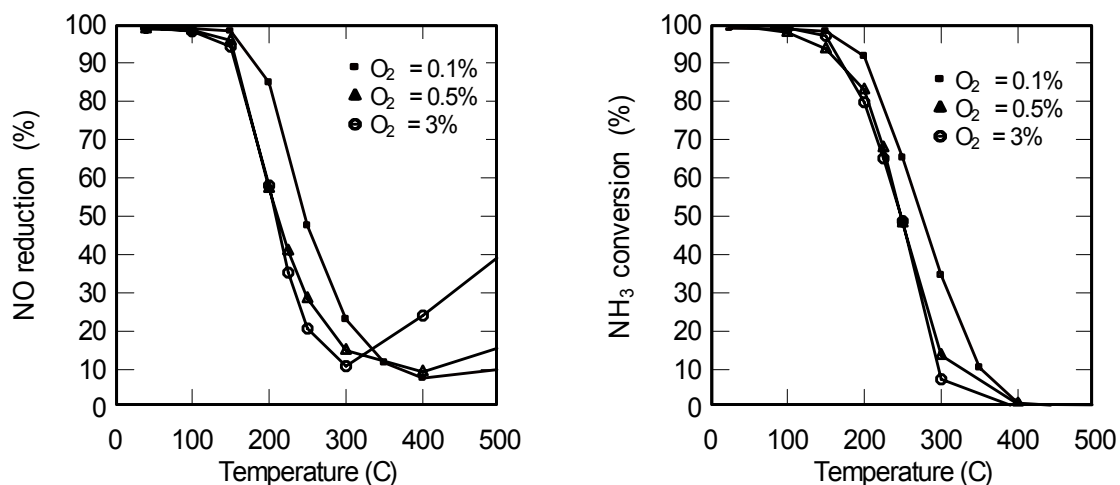
Figure 29. NO reduction and NH₃ conversion at different oxygen concentrations using Cu-ZSM-5. The reaction conditions are: NO = 330 ppm, NH$_3$ = 330 ppm, NH$_3$-to-NO ratio = 1.0, SV = 42000 hr^{-1}, with pretreatment with H$_2$.

ture around 300°C and for a certain duration of time (e.g., 1 hr). Pretreatment with hydrogen did not produce a significant difference in the results for both NO reduction and NH$_3$ conversion. This could be attributed to the copper loading on the catalyst, which was only 5%, by weight. As listed in Table 5, the pretreated catalyst was used at two space velocities, 7000 hr^{-1} and 42000 hr^{-1}, and at two NH$_3$-to-NO ratios, 0.8 and 1.0. Results are shown in Figures 28–30.
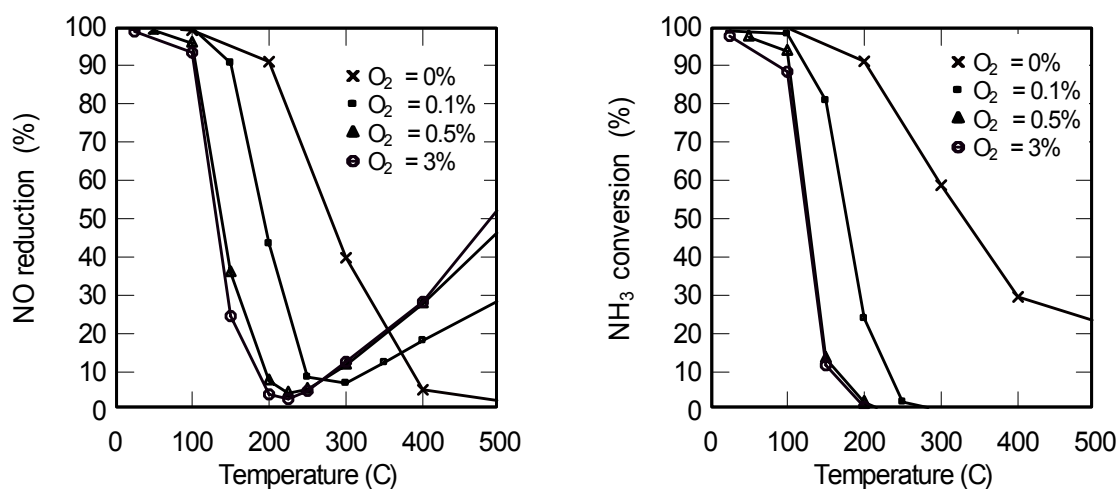
Figure 30. NO reduction and NH₃ conversion at different oxygen concentrations using Cu-ZSM-5. The reaction conditions are: NO = 330 ppm, NH$_3$ = 330 ppm, NH$_3$-to-NO ratio = 1.0, SV = 7000 hr^{-1}, with pretreatment with H$_2$.

6.1.5 N_2O and NO_2 generation

Similar to the results in the above sections for NO reduction and NH_3 conversion using the Cu-ZSM-5 catalyst, the effect of different parameters on N_2O and NO_2 generation will be presented in this section. In Figure 31, the effect of oxygen concentration on N_2O and NO_2 generation is shown at a given space velocity. At higher O_2 concentrations, more generation of NO_2 takes place than N_2O. Though a higher oxygen concentration seems to favor higher generation for both. Typically, the peak N_2O concentration is obtained at the temperature where peak NO reduction occurs. This however, cannot be said about NO_2. Apparently, the reduction in NO is accompanied with the generation of N_2O at higher oxygen concentrations.
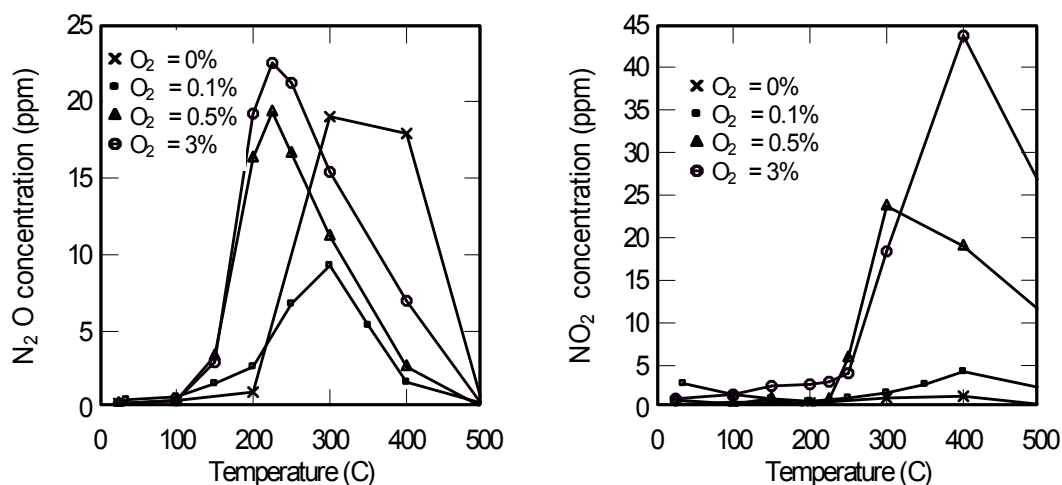
Figure 31. Effect of O_2 on N_2O and NO_2 generation using Cu-ZSM-5. The reaction conditions are: NO = NH_3 = 330 ppm, SV = 7000 hr^{-1}, without pretreatment with H_2.

Figures 32 and 33, in combination with Figure 31, show the effect of space velocity on N_2O and NO_2 generation. Though the N_2O concentration decreases slightly with an increase of space velocity, the NO_2 concentration seems to slightly increase with space velocity. Note the change in scale for the NO_2 concentration in Figure 33.

Figure 32. N_2O and NO_2 generation using Cu-ZSM-5. The reaction conditions are: NO = NH_3 = 330 ppm, SV = 42000 hr^{-1}, without pretreatment with H_2.
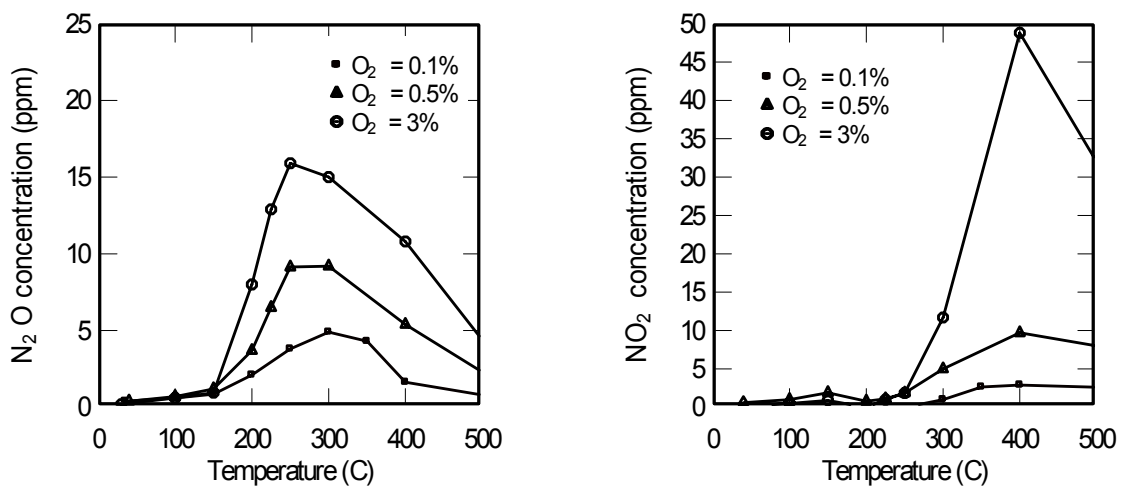
Figure 33. N_2O and NO_2 generation using Cu-ZSM-5. The reaction conditions are: NO = NH_3 = 330 ppm, SV = 64000 hr^{-1}, without pretreatment with H_2.

Figures 34 and 35 show the effect of NH_3-to-NO ratio on N_2O and NO_2 generation at a space velocity of 42000 hr^{-1}. In combination with Figure 32, results can be seen for the entire range of variation of NH_3-to-NO ratios from 0.8 to 2.0. Presence of more ammonia seems to fa-

vor N$_2$O generation, whereas decreases the generation of NO$_2$. Note the change in scale for the figures showing NO$_2$ concentration (Figure 34) and N$_2$O concentration (Figure 35).
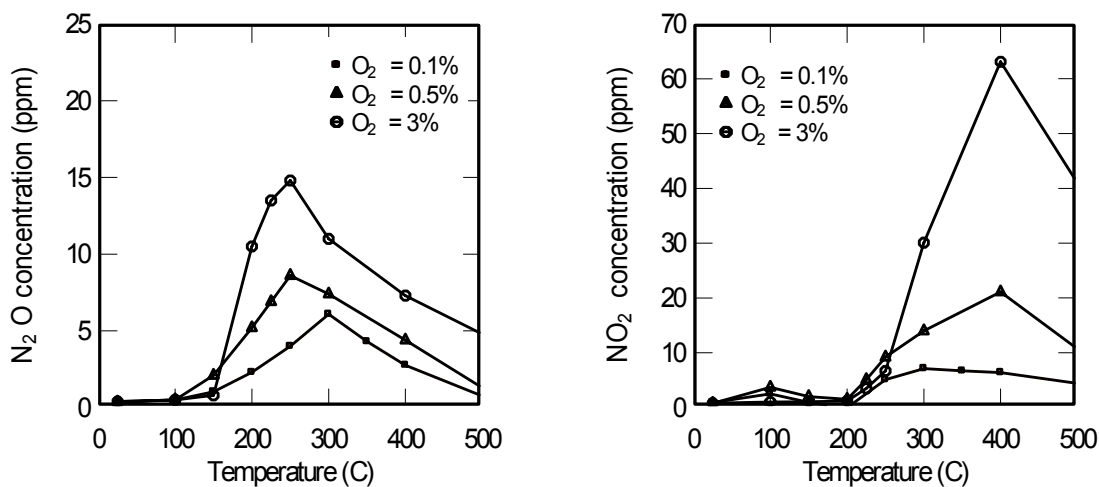
Figure 34. N$_2$O and NO$_2$ generation using Cu-ZSM-5. The reaction conditions are: NO = 330 ppm, NH$_3$ = 264 ppm, NH$_3$–to-NO ratio = 0.8, SV = 42000 hr^{-1}, without pretreatment with H$_2$.
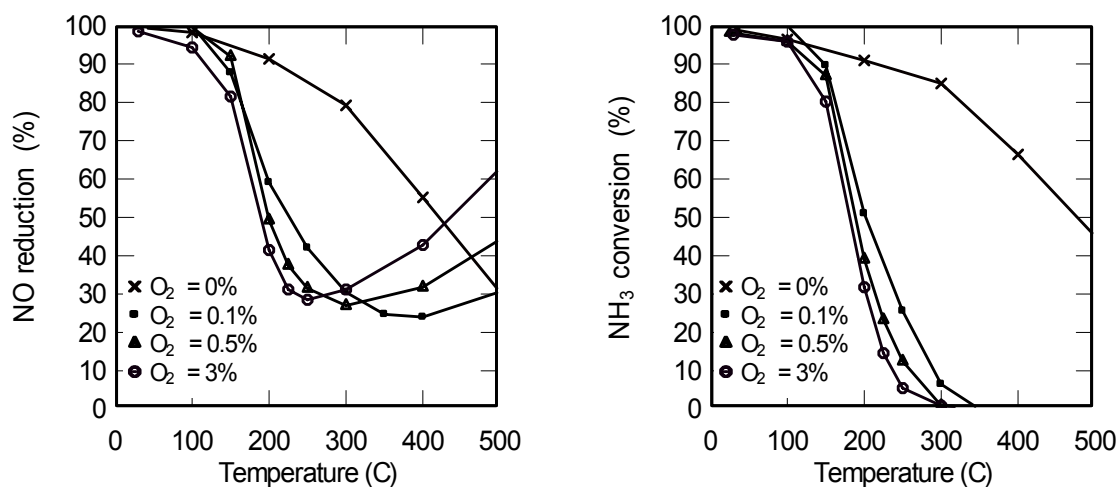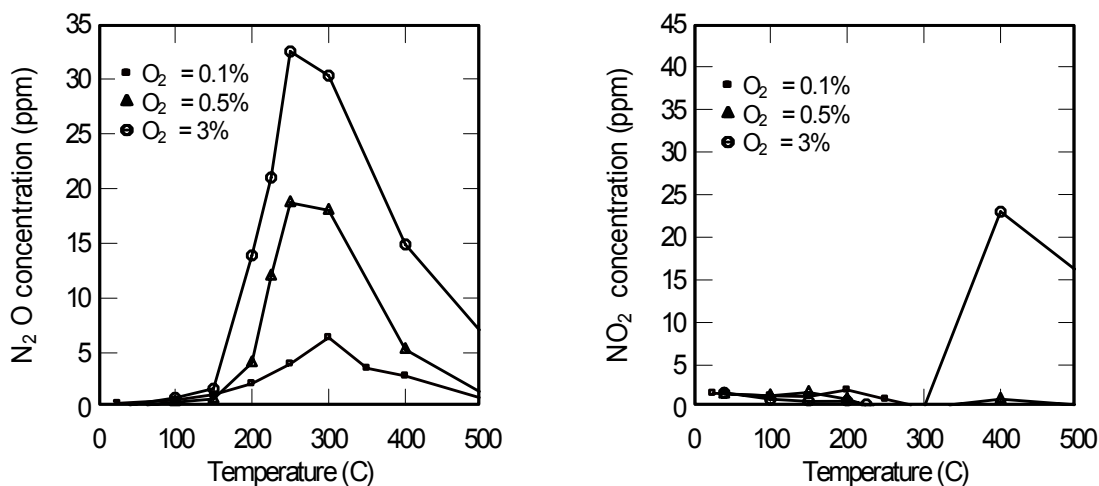

Figure 35. N$_2$O and NO$_2$ generation using Cu-ZSM-5. The reaction conditions are: NO = 330 ppm, NH$_3$ = 660 ppm, NH$_3$–to-NO ratio = 2.0, SV = 42000 hr^{-1}, without pretreatment with H$_2$.

Figures 36–37 show the effect of pretreatment with hydrogen on N_2O and NO_2 genera-tion. Similar to the case with NO reduction and NH_3 conversion, pretreatment with hydrogen does not seem to bring a particular pattern to the change in results when compared with results for cases without any pretreatment. Figure 36 upon comparison with Figure 31 seems to suggest that pretreatment tends to increase both N_2O and NO_2 generations. However, Figure 37 upon comparison with Figure 32 shows a decrease in both N_2O and NO_2 generations.
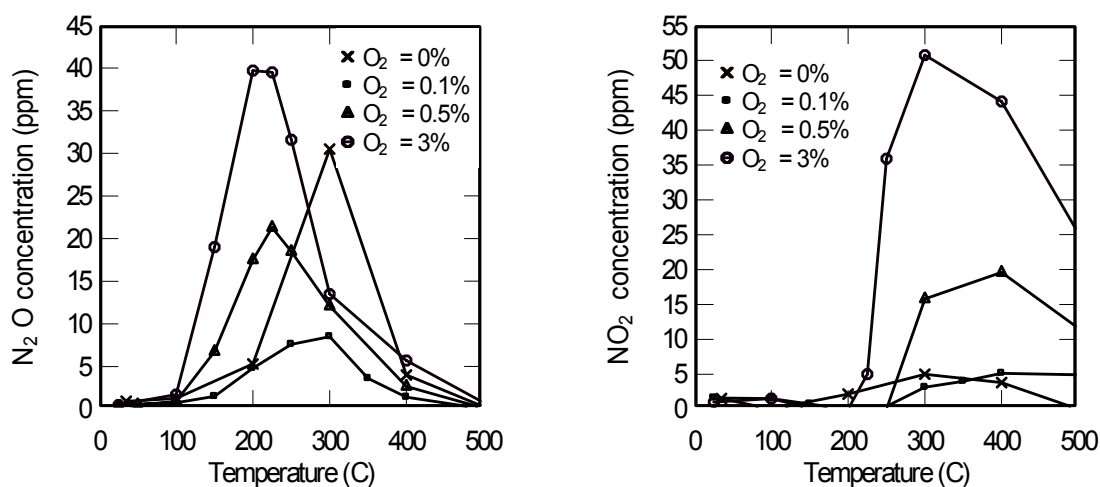
Figure 36. N_2O and NO_2 generation using Cu-ZSM-5. The reaction conditions are: NO = NH_3 = 330 ppm, SV = 7000 hr^{-1}, with pretreatment with H_2.
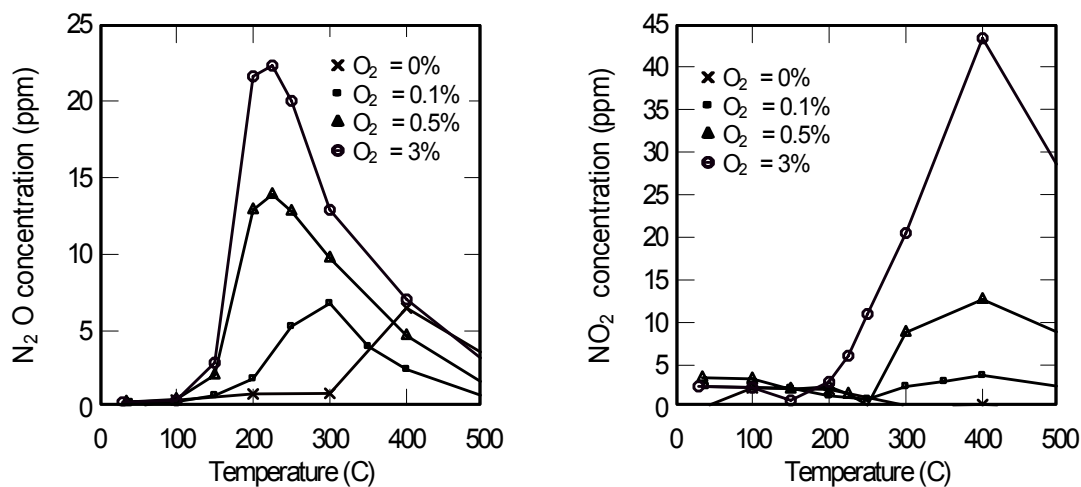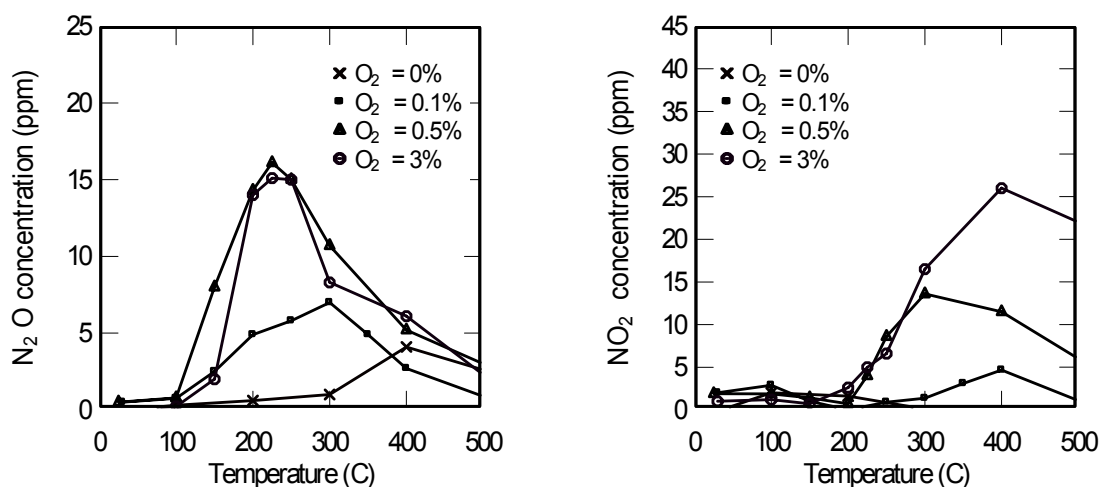

Figure 37. N_2O and NO_2 generation using Cu-ZSM-5. The reaction conditions are: NO = NH_3 = 330 ppm, SV = 42000 hr^{-1}, with pretreatment with H_2.

6.2 Using Va-based catalyst

Table 6 lists the experimental cases performed on vanadium-based catalyst supported on cordierite ceramic honeycomb. Unlike the experimental cases done for the Cu-ZSM-5 catalyst, the listed cases cater to the variation in only three parameters: oxygen concentration, space velocity (SV), and NH_3-to-NO ratio. No pretreatment with hydrogen was done for any of the cases.

Table 6. Experimental cases performed on Va-based
honeycomb monolith catalyst.

$NH_3 = 264$ ppm	SV = 42000 hr^{-1}	$O_2 = 0.1$ %
		$O_2 = 0.5$ %
		$O_2 = 3$ %
$NH_3 = 330$ ppm	SV = 7000 hr^{-1}	$O_2 = 0.1$ %
		$O_2 = 0.5$ %
		$O_2 = 3$ %
	SV = 42000 hr^{-1}	$O_2 = 0$ %
		$O_2 = 0.1$ %
		$O_2 = 0.5$ %
		$O_2 = 3$ %
	SV = 64000 hr^{-1}	$O_2 = 0.1$ %
		$O_2 = 0.5$ %
		$O_2 = 3$ %
$NH_3 = 660$ ppm	SV = 42000 hr^{-1}	$O_2 = 0.1$ %
		$O_2 = 0.5$ %
		$O_2 = 3$ %

6.2.1 Effect of O_2 concentration

Figures 38 and 39 show the effect of inlet oxygen concentration on the NO reduction and NH_3 conversion, respectively. The experimental conditions were: NO = NH_3 = 330 ppm, SV = 7000 hr^{-1}. As per the figures, an increase in oxygen concentration not only increases the peak NO reduction, but also slightly lowers the temperature for complete NH_3 conversion; both of

Figure 38. NO reduction at different oxygen concentrations using Va-based catalyst. The reaction conditions are: $NO = NH_3 = 330$ ppm, $SV = 7000$ hr^{-1}.

Figure 39. NH$_3$ conversion at different oxygen concentrations using Va-based catalyst. The reaction conditions are: $NO = NH_3 = 330$ ppm, $SV = 7000$ hr^{-1}.

which are desirable. A higher NO reduction means the removal of more NO from the exhaust, and lower temperature for complete NH_3 conversion means the elimination of any residual ammonia. Note the decrease in the temperature range at which higher NO reduction is obtained with an increase in oxygen concentration. At around 500°C more NO is generated than being fed into the reactor.

6.2.2 Effect of space velocity

Figures 40 and 41 show the NO reduction and NH_3 conversion at space velocities (SV) of 42000 hr^{-1} and 64000 hr^{-1}, respectively. These two figures can be observed together with the Figures 38 and 39 for a complete comparison of the results over the entire range of space velocities, from 7000 to 64000 hr^{-1}.

An increase in space velocity increases the residual ammonia at higher temperatures (around 500°C). Though complete NH_3 conversion is obtained at around 350–400°C, for a lower space velocity of 7000 hr^{-1}, more than 10% of the supplied amount of NH_3 is still left even at 500°C for the higher space velocity of 64000 hr^{-1}.

A decrease in the extent of NO reduction is observed as the space velocity is increased, with the highest NO reduction of around 90% being observed at a space velocity of 7000 hr^{-1}. Also an increase in the residual ammonia at 500°C is observed as the space velocity increases. The variation in the extent of NO reduction with space velocity is quantified in Figure 42. Irrespective of the oxygen concentration, the extent of NO reduction successively decreases as the space velocity is increased.

Figure 40. NO reduction and NH_3 conversion at different oxygen concentrations using Va-based catalyst. The reaction conditions are: NO = NH_3 = 330 ppm, SV = 42000 hr^{-1}.
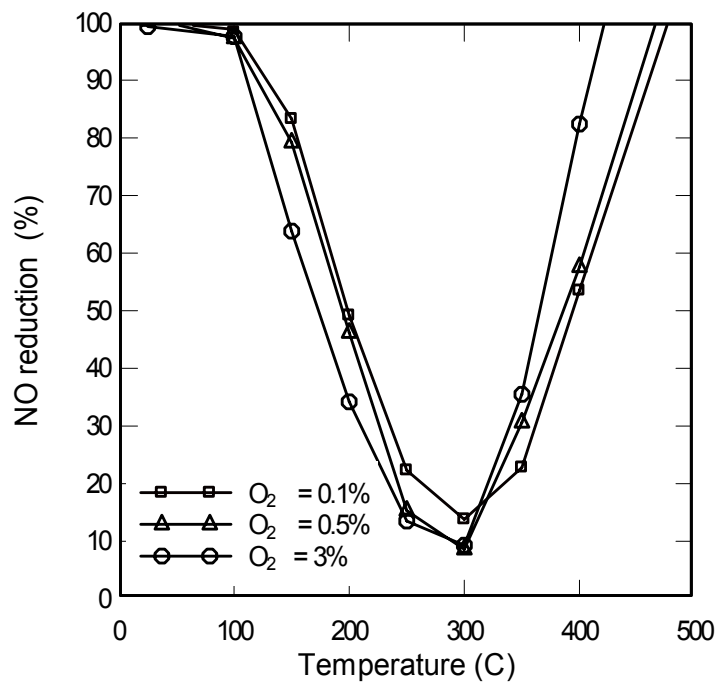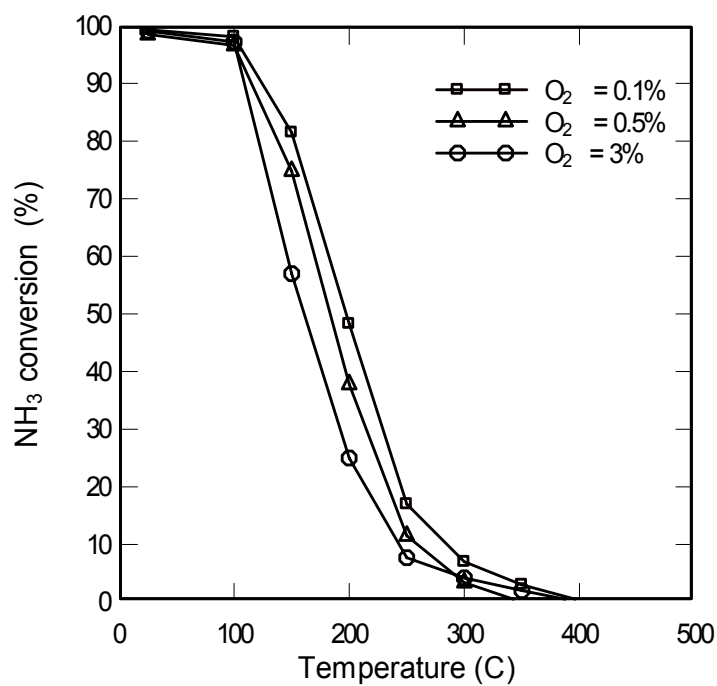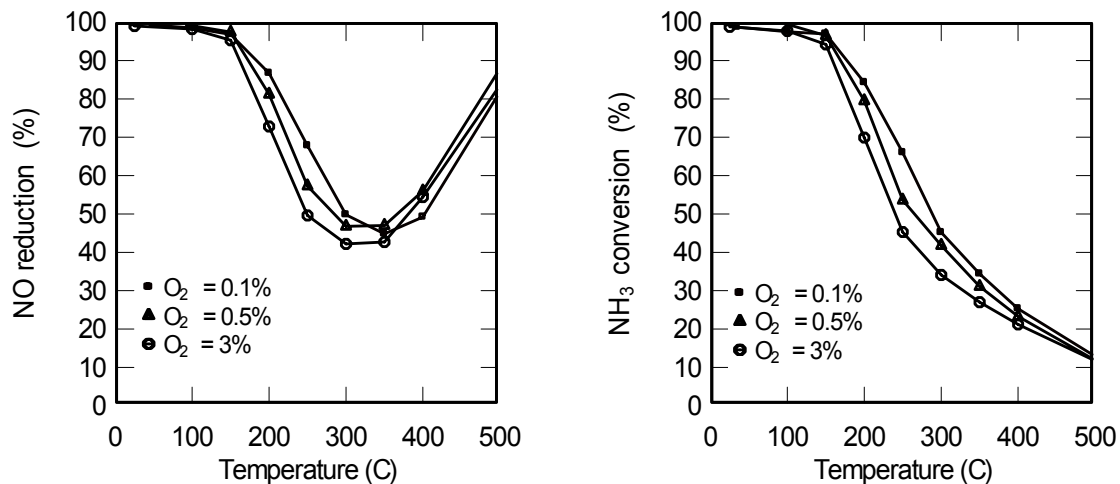
Figure 41. NO reduction and NH_3 conversion at different oxygen concentrations using Va-based catalyst. The reaction conditions are: NO = NH_3 = 330 ppm, SV = 64000 hr^{-1}.

Figure 43 shows the effect of space velocity on the temperature at which peak NO reduction is obtained. The required temperature for peak NO reduction rises with the space velocity. At the higher oxygen concentrations, 0.5% and 3%, the required temperature is lower than that for an oxygen concentration of 0.1%, at all space velocities, indicating that a leaner mixture favors higher NO reduction at lower temperatures.
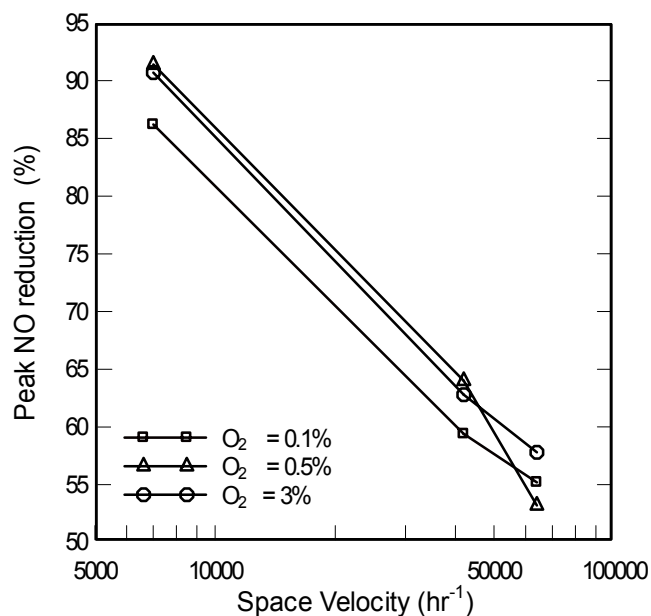
Figure 42. Variation in peak NO reduction with space velocity at different oxygen concentrations using Va-based catalyst. The reaction conditions are: NO = NH_3 = 330 ppm.

Figure 43. Variation in temperature for peak NO reduction with space velocity at different oxygen concentrations using Va-based catalyst. The reaction conditions are: NO = NH$_3$ = 330 ppm.

6.2.3 Effect of ammonia concentration

As the third parameter to be analyzed, the inlet NH$_3$ concentration fed into the reactor was varied at a space velocity of 42000 hr^{-1}. The results are shown in Figures 44 and 45. The two
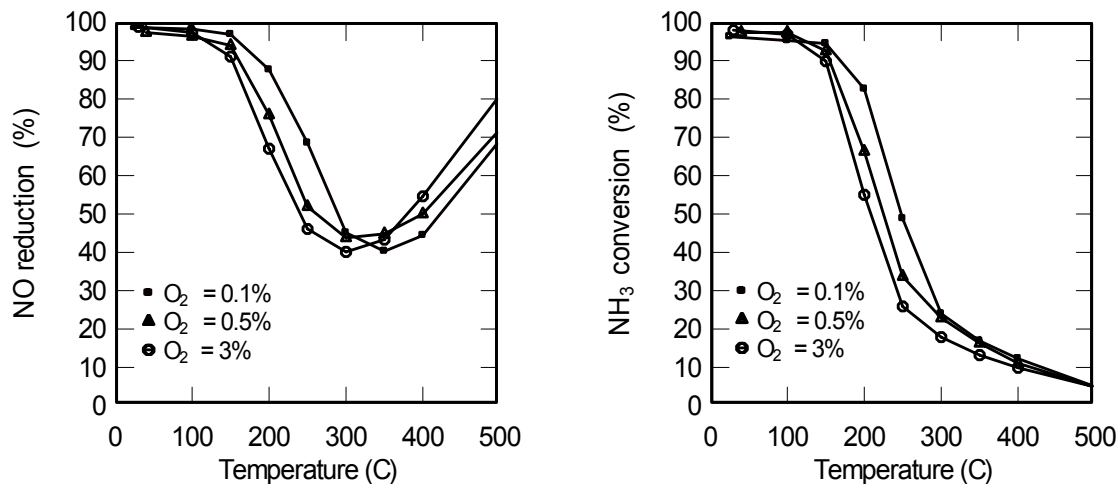
Figure 44. NO reduction and NH$_3$ conversion at different oxygen concentrations using Va-based catalyst. The reaction conditions are: NO = 330 ppm, NH$_3$ = 264 ppm, NH$_3$-to-NO ratio = 0.8, SV = 42000 hr^{-1}.
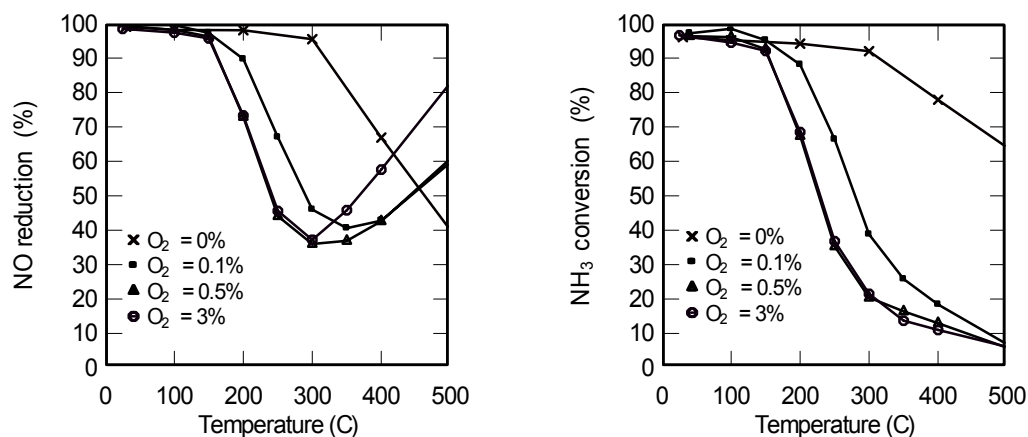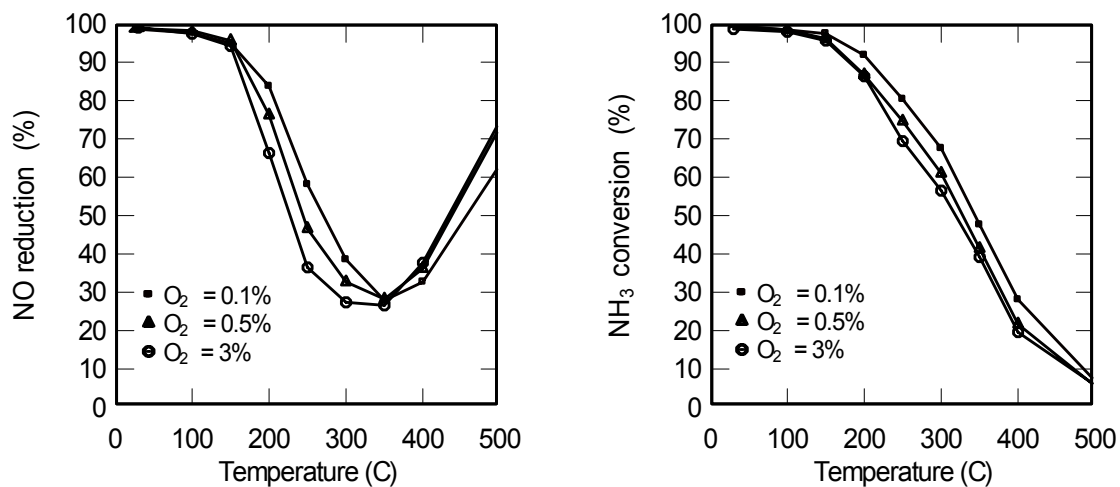
Figure 45. NO reduction and NH$_3$ conversion at different oxygen concentrations using Va-based catalyst. The reaction conditions are: NO = 330 ppm, NH$_3$ = 660 ppm, NH$_3$-to-NO ratio = 2.0, SV = 42000 hr^{-1}.

figures can be analyzed together with Figure 40 for the complete comparison of the effect of variation in NH$_3$-to-NO ratio from 0.8 to 2.0. At a given space velocity, an increase in the NH$_3$-to-NO ratio favors higher NO reduction. However, an increase in residual ammonia at a tempera-
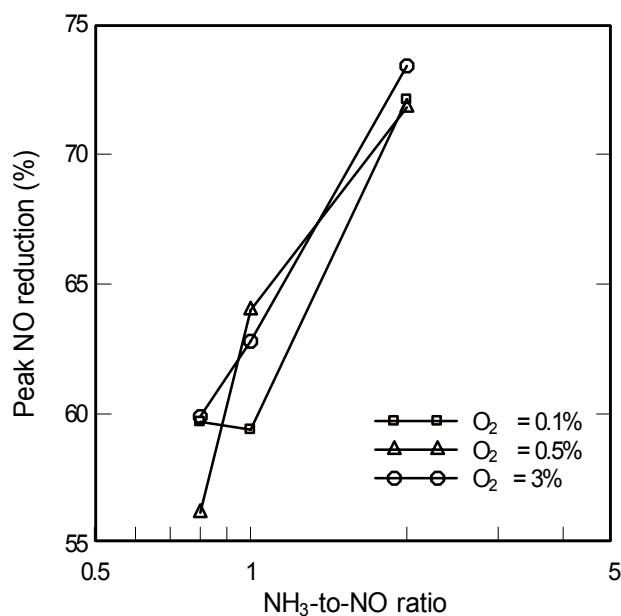
Figure 46. Variation in peak NO reduction with NH$_3$-to-NO ratio at different oxygen concentrations using Va-based catalyst at space velocity of 42000 hr^{-1}.

ture of 500°C is also observed. Note that 10% residual ammonia at NH_3-to-NO ratio of 2.0 (inlet NH_3 = 660 ppm) is much higher than the same percentage at NH_3-to-NO ratio of 0.8 (inlet NH_3 = 264 ppm). The nature of variation of peak NO reduction with NH_3-to-NO ratio is quantified in Figure 46. The peak NO reduction continuously improves from around 55% to around 75%. The eliminated NO converts itself primarily to N_2, accompanied with some N_2O and NO_2.

Another parameter of interest is the variation in the temperature at which peak NO reduction occurs with the variation in NH_3-to-NO ratio. This result is shown in Figure 47. Though a higher NH_3-to-NO ratio improves the peak NO reduction, the temperature at which the peak NO reduction occurs also increases simultaneously (though a variation in NH_3-to-NO ratio from 0.8 to 1.0 does not seem to affect the temperature). This is true irrespective of the inlet oxygen concentration.
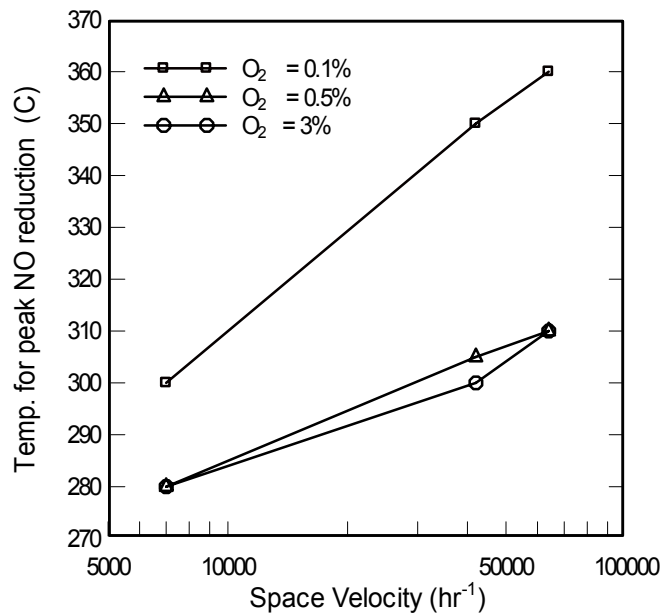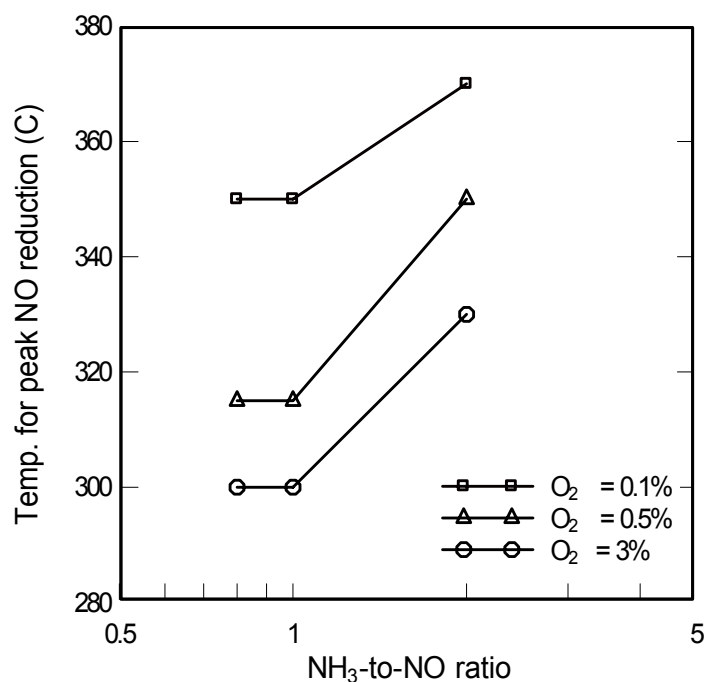

Figure 47. Variation in temperature for peak NO reduction with NH_3-to-NO ratio at different oxygen concentrations using Va-based catalyst at space velocity of 42000 hr^{-1}.

An increase in NH_3-to-NO ratio tends to increase the residual ammonia left even at higher temperatures. This nature of the result is shown in Figure 48 for the vanadium-based cata-

lyst at a space velocity of 42000 hr^{-1}. A higher oxygen concentration tends to favor lower residual ammonia. Though not a significant difference is obtained when the oxygen concentration is increased from 0.5 to 3%.
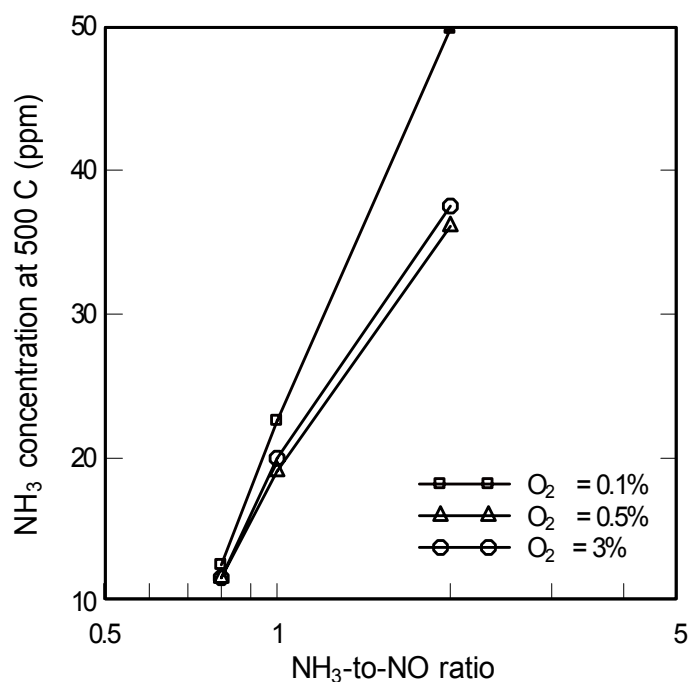
Figure 48. Variation in NH_3 concentration at 500°C with NH_3-to-NO ratio at different oxygen concentrations using Va-based catalyst at space velocity of 42000 hr^{-1}.

6.2.4 N_2O and NO_2 generation

Similar to the results for the Cu-ZSM-5 catalyst, the effect of different parameters on the generation of N_2O and NO_2 species for the vanadium-based catalyst will be presented in this section. Figure 49 shows the results for the effect of oxygen on N_2O and NO_2 generation. Though a high oxygen concentration decreases the generation of N_2O, it increases NO_2 generation. The concentration of N_2O decreases at higher temperatures, after reaching a peak value, irrespective of the oxygen concentration. The concentration of NO_2 on the other hand, increases rapidly at high temperatures. This increase is significantly marked for cases with high inlet oxygen concentrations.
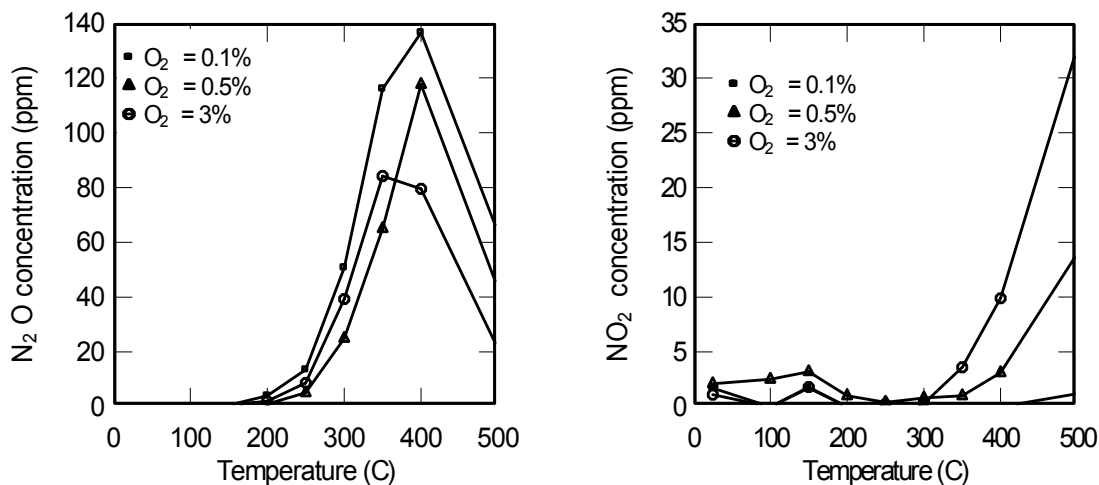
Figure 49. Effect of O_2 on N_2O and NO_2 generation using Va-based catalyst. The reaction conditions are: $NO = NH_3 = 330$ ppm, $SV = 7000$ hr^{-1}.

In Figures 50 and 51, the effect of space velocity on the generation of N_2O and NO_2 is shown. An increase in space velocity tends to reduce the generation of N_2O, irrespective of the concentration of oxygen. And at higher space velocities, the generation of NO_2 is virtually eliminated. A concentration of less than 3 ppm can be safely assumed to be an uncertainty in experimental measurement.
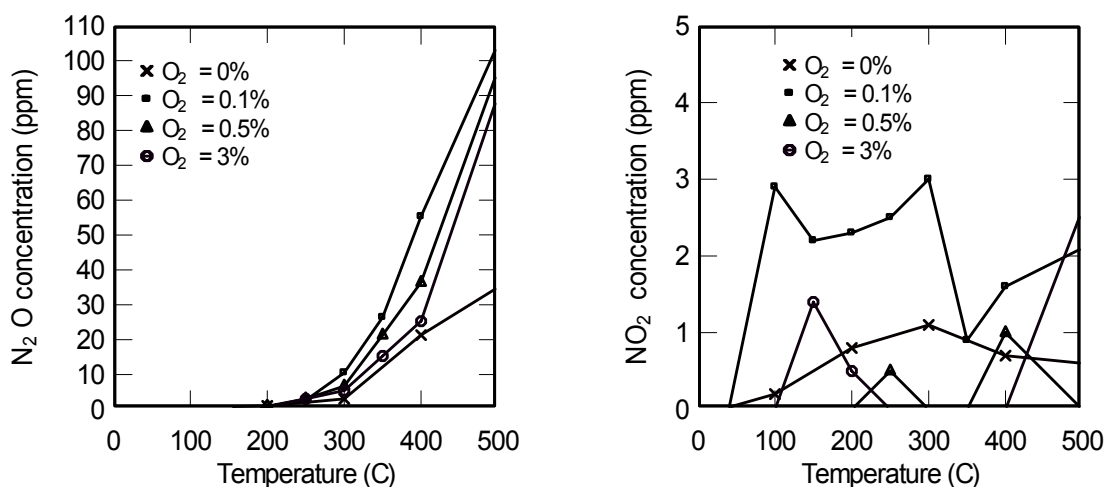
Figure 50. N_2O and NO_2 generation using Va-based catalyst. The reaction conditions are: $NO = NH_3 = 330$ ppm, $SV = 42000$ hr^{-1}.
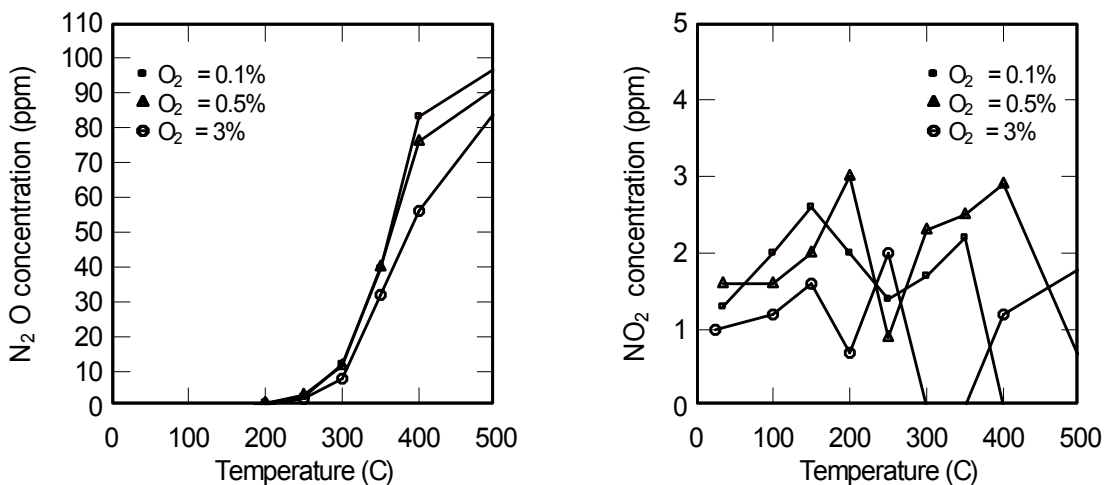
Figure 51. N_2O and NO_2 generation using Va-based catalyst. The reaction conditions are: $NO = NH_3 = 330$ ppm, $SV = 64000$ hr^{-1}.

Figures 52 and 53 show the effect of variation of NH_3-to-NO ratio on the generation of N_2O and NO_2. An increase in inlet NH_3-to-NO ratio increases the generation of N_2O. Note the change in scale for the N_2O concentration in Figure 53. It however, has no effect on NO_2. The NO_2 specie is virtually absent irrespective of the NH_3-to-NO ratio.

Figure 52. N_2O and NO_2 generation using Va-based catalyst. The reaction conditions are: $NO = 330$ ppm, $NH_3 = 264$ ppm, NH_3–to-NO ratio = 0.8, $SV = 42000$ hr^{-1}.

Figure 53. N$_2$O and NO$_2$ generation using Va-based catalyst. The reaction conditions are: NO = 330 ppm, NH$_3$ = 660 ppm, NH$_3$–to-NO ratio = 2.0, SV = 42000 hr^{-1}.

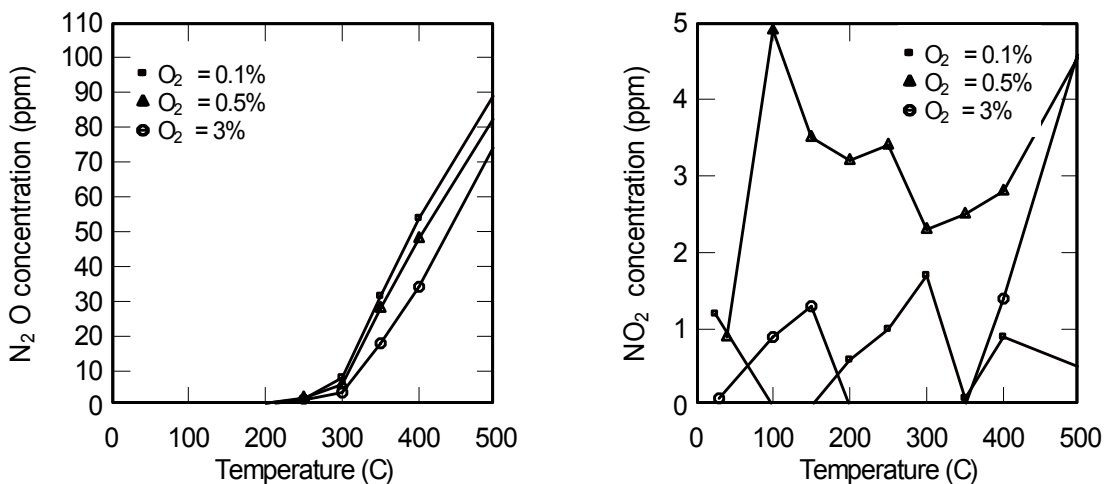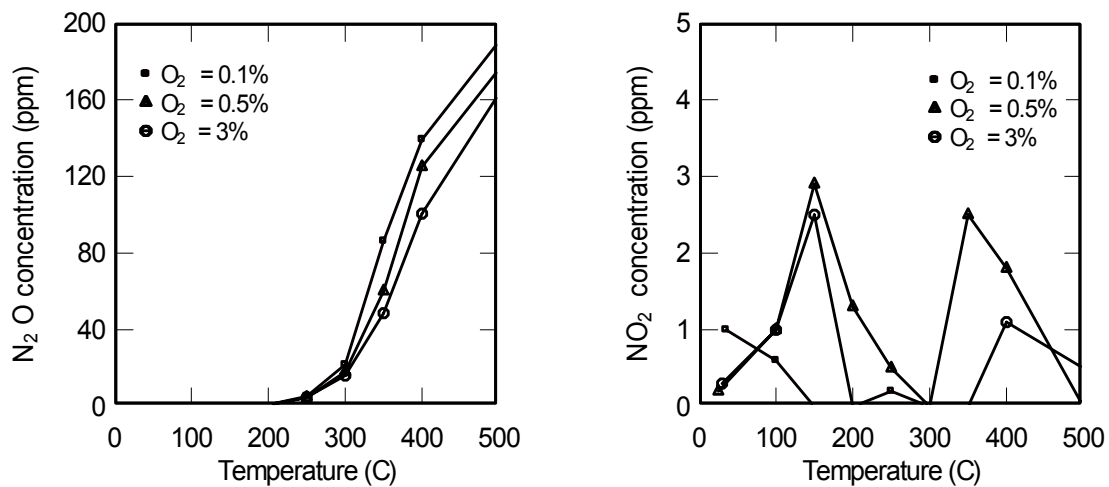# 7. SUMMARY, CONCLUSIONS AND RECOMMENDATIONS

The two catalyst samples: zeolite-based (Cu-ZSM-5) and vanadium-based, were investigated for the removal of nitric oxide (NO) using ammonia (NH_3) from exhaust streams in a laboratory laminar-flow reactor. The experiments used a number of gas compositions to simulate different combustion gases. The gases were heated from ambient temperature to 500°C.

The effects of four parameters were investigated for the zeolite-based Cu-ZSM-5 catalyst. The results can be summarized as below:

- The inlet oxygen concentration was varied from 0 to 3%. An increase in oxygen concentration, from 0.1 to 3%, reduced the temperatures at which peak NO reduction and complete NH_3 conversion were obtained, and had no effect on the extent of NO reduction. However, an accompanied increase in the concentrations of both N_2O and NO_2 species was observed. The concentration of NO_2 increased (with inlet O_2 concentration) up to a value of 50 ppm at an O_2 concentration of 3% (SV = 64000 hr^{-1}, without H_2 pretreatment).

- Space velocity, the second parameter to be varied, is defined as the volume ratio of gas flow rate relative to the catalyst volume, expressed in per-hour. An increase in space velocity (from 7000 to 64000 hr^{-1}) decreased the peak NO reduction, from around 95% to as low as 75%, irrespective of the O_2 concentration. It also increased the temperature at which complete NH_3 conversion was obtained. However, an increase in space velocity was accompanied by a slight decrease in N_2O concentration (from around 25 to 15 ppm) and it had no effect on NO_2 concentration (which remained around 45 ppm).

- NH_3-to-NO ratio was varied from 0.8 (NH_3 = 264 ppm, NO = 330 ppm) to 2.0 (NH_3 = 660 ppm, NO = 330 ppm). This increase in NH_3-to-NO ratio increased the peak NO reduction from around 67 to 92% (SV = 42000 hr^{-1}, without pretreatment with H_2), irrespective of the O_2 concentration. However, an accompanied increase in the temperature for complete NH_3 removal and the concentration of N_2O specie was also observed.

- Pretreatment, the last parameter to be varied, refers to the process of exposing the catalyst to only a particular gas, in our case hydrogen, at the flow rate of 1100 sccm. This step was performed for a time duration of 1 hour while keeping the reactor at a temperature of 300°C. Pretreatment with hydrogen did not produce a significant difference in the results for both NO reduction and NH_3 conversion. This could be attributed to the lower degree of copper loading on the catalyst, which was only 5%, by weight.

For the vanadium-based catalyst, the effects of variation of three parameters were investigated (unlike the Cu-ZSM-5 catalyst). The results can be summarized as follows:

- An increase in oxygen concentration (from 0.1 to 3%) reduced the temperature at which peak NO reduction was obtained, and slightly improved the peak NO reduction. This was, however, accompanied with a decrease in the concentration of N_2O and an increase in NO_2 concentration. At a space velocity of 7000 hr^{-1}, the N_2O concentration decreased from 140 to 80 ppm and NO_2 concentration increased from around 14 to 32 ppm when the oxygen concentration was raised from 0.1 to 3%.

- Increase in space velocity (from 7000 to 64000 hr^{-1}) decreased the peak NO reduction, from around 95% to as low as 60%, irrespective of the O_2 concentration. It also increased the amount of residual NH_3 at 500°C. However, an accompanied decrease in N_2O concentration (from around 140 to 90 ppm) and complete elimination of NO_2 was also observed.

- An increase in NH_3-to-NO ratio from 0.8 to 2.0 increased the peak NO reduction from around 60 to 75% (SV = 42000 hr^{-1}). However, an accompanied increase in the residual ammonia (at 500°C) and N_2O concentration (from around 85 to 180 ppm) was also observed, irrespective of the O_2 concentration.

Overall, the Cu-ZSM-5 catalyst was more effective for NO reduction than the vanadium-based catalyst. Under identical conditions of O_2 and NH_3 concentrations and space velocity, a higher NO reduction and NH_3 removal, with lower generation of N_2O and NO_2 species was obtained for the Cu-ZSM-5 catalyst.

The recommendations for future work are listed as below:

- The effect of the presence of water (H_2O) needs to be investigated for the zeolite-based (Cu-ZSM-5) catalyst sample.

- Effect of variation in copper-loading (by weight %) on NO reduction when the Cu-ZSM-5 catalyst sample is pretreated with H_2 needs to be investigated.

- The effect of a combination of SNCR and SCR experimental set-up (e.g. heating Zone-3 of the furnace to 1000°C and Zone-2 with Zone-1 to around 500°C, with the catalyst sample placed somewhere near the boundary between Zone-2 and Zone-1) can be investigated.

- Other varieties of promising catalysts, e.g. Pillared Layer Catalysts (PiLCs), can be investigated in the SCR process.

REFERENCES

1. Cheung, T., Bhargava, S. K., Hobday, M., and Foger, K., 1996, "Adsorption of NO on Cu Exchanged Zeolites, an FTIR Study: Effects of Cu Levels, NO Pressure and Catalyst Pre-treatment," Journal of Catalysis, **158**, pp. 301–310.

2. Clarke, A. G., Radojevic, M., and Harrison, R. M., 1992, *Atmospheric Acidity: Sources, Consequences and Abatement*, Elsevier, London.

3. Bowman, C. T., 1992, "Control of Combustion-Generated Nitrogen Oxide Emissions; Technology Driven by Regulation," Twenty-Fourth Symposium (International) on Combustion, The Combustion Institute, Pittsburgh, PA, pp. 859–878.

4. Albanese, V., Kellogg, G., and Eisenmann, D.R., 1994, "The Clean Air Advisor," Nalco/Fuel Tech, **3**(2), pp. 1–6.

5. Mincy, J. E., 1992, "Controlling NO_x to Obtain Offsets of Meet Compliance," Fourteenth National Industrial Energy Technology Conference, Houston, TX, pp. 173–176.

6. National Aeronautics and Space Administration (NASA) Facts, 1998, "Ozone: What Is It, and Why Do We Care about It," Cape Girardeau, MO, NF–198.

7. Heywood, John B., 1988, *Internal Combustion Engine Fundamentals*, McGraw-Hill, New York.

8. "Prediction of NO_x Emissions in Recovery Boilers' – An Introduction to NO_x Module," Available: http://www.psl.bc.ca/downloads/ftp/kilns/Model-NOx.pdf, Accessed: 02/08/2003.

9. Glarborg, P., Miller, J. A., and Kee, R. J., 1986, "Kinetic Modeling and Sensitivity Analysis of Nitrogen Oxide Formation in Well-Stirred Reactors," Combust. Flame, **65,** pp. 177–202.

10. "NO_X Formation Literature Review and Research Project," Available: http://ecosse.org/jack/Projects/proj2000/degussa/degussa.html, Accessed: 02/08/2003.

11. Miller, J. A., and Bowman, C. T., 1989, "Mechanisms and Modeling of Nitrogen Chemistry in Combustion," Prog. Energy Combust. Sci., **15**, pp**.** 287–338.

12. Eastwood, P., 2000, *Critical Topics in Exhaust Gas After-treatment*, Research Studies Press, London.

13. Radojevic, M., 1998, "Reduction of Nitrogen Oxides in Flue Gases," Environmental Pollution, **102**, S1, pp. 685–689.

14. Lyon, R. K., and Hardy, J. E., 1986, "Discovery and Development of the Thermal $DeNO_x$ Process," Ind. Eng. Chem. Fundam., **25**, pp. 19–24.

15. Breck, D. W., 1974, *Zeolite Molecular Sieves: Structure, Chemistry and Use*, Wiley, New York.

16. Larsen, S. C., Aylor, A., Bell, A. T., and Reimer, J. A., 1994, "Electron Paramagnetic Resonance Studies of Copper Ion-Exchanged ZSM-5," J. Phys. Chem., **98**, pp. 11533–11540.

17. Sun, T., Fokema, M. D., and Ying, J. Y., 1997, "Mechanistic Study of NO Reduction with Methane over Co^{2+} Modified ZSM-5 Catalysts," Catalysis Today, **33**, pp. 251–261.

18. Konno, M., Chikahisa, T., Murayama, T., and Iwamoto, M., 1992, "Catalytic Reduction of NO_x in Actual Diesel Exhaust," Society of Automotive Engineers, SAE 920091.

19. Roozeboom, F., Moulijn, J. A., Medema, J., and Gellings, P. J., 1980, "Vanadium Oxide Monolayer Catalysts," J. Phys. Chem., **84**, pp. 2783–2791.

20. Wachs, I. E., and Weckhuysen, B.M., 1997, "Structure and Reactivity of Surface Vanadium Oxide Species on Oxide Supports," Applied Catalysis A: General, **157**, pp. 67–90.

21. Iwamoto, M., Yahiro, H., Mizuno, N., Zhang, W., Mine, Y., Furukawa, H., and Kagawa, S., 1992, "Removal of Nitric Oxide through a Novel Catalytic Process," J. Phys. Chem., **96**, pp. 9360–9366.

22. Komatsu, T., Nunokawa, M., Moon, I. S., Takahara, T., Namba, S., and Yashima, T., 1994, "Kinetic Studies of Reduction of Nitric Oxide with Ammonia on Cu^{2+}-Exchanged Zeolites," Journal of Catalysis, **148**, pp. 427–437.

23. Sullivan, J. A., and Cunningham, J., 1998, "Selective Catalytic Reduction of NO with C_2H_4 over Cu-ZSM-5: Influences of Oxygen Partial Pressure and Incorporated Rhodia," Applied Catalysis B: Environmental, **15**, pp. 275–289.

24. Cho, B. K., 1993, "Nitric Oxide Reduction by Hydrocarbons over Cu-ZSM-5 Monolith Catalyst under Lean Conditions: Steady-state Kinetics," Journal of Catalysis, **142**, pp. 418–429.

25. Long, R.Q., and Yang, R.T., 2001, "Selective Catalytic Oxidation of Ammonia to Nitrogen over Fe-Exchanged Zeolites," Journal of Catalysis, **201**, pp. 145–152.

26. Curtin, T., Grange, P., and Delmon, B., 1997, "The Effect of Pretreatments on Different Copper Exchanged ZSM-5 for the Decomposition of NO," Catalysis Today, **36**, pp. 57–64.

27. Bosch, F., and Janssen, F., 1988, "Formation and Control of Nitrogen Oxides," Catalysis Today, **2**, pp. 369–532.

28. Parvlescu, V. I., Grange, P., and Delmon, B., 1998, "Catalytic Removal of NO," Catalysis Today, **46**, pp. 233–316.

29. Liuqing, T., Daiqi, Y., and Hong, L., 2003, "Catalytic Performance of a Novel Ceramic-Supported Vanadium Oxide Catalyst for NO Reduction with NH_3," Catalysis Today, **78**, pp. 159–170.

30. Gentemann, A., 2001, "Flow Reactor Experiments on the Selective Non-Catalytic Removal of Nitrogen Oxides," M.S. Thesis, Texas A&M University, College Station, Texas.

31. Mangan, J., 2000, "The Calibration and Use of Mass Flow Controllers for Use in NO_x Reduction Experiments," MEEN 485 Report, Texas A&M University, College Station, Texas.

32. Park, Y., 2003, "An Investigation of Urea Decomposition and Selective Non-Catalytic Removal of Nitric Oxide with Urea," M.S. Thesis, Texas A&M University, College Station, Texas.

APPENDIX 1

CALIBRATION OF MASS FLOW CONTROLLERS

For the calibration of the mass flow controllers, a thermometer to measure water and ambient temperature, a ruler to measure the height of water level, a stop-watch to measure time, flasks and a basin to contain H_2O were required. As a first step of the calibration, MFC was turned on and allowed to warm up and water was added to the basin. After the above step was completed, the value read by the MFC was checked to confirm that no gas is flowing at zero setting. Then, the MFC was set to a chosen value as per the planning to take a total of five to six flow measurements.
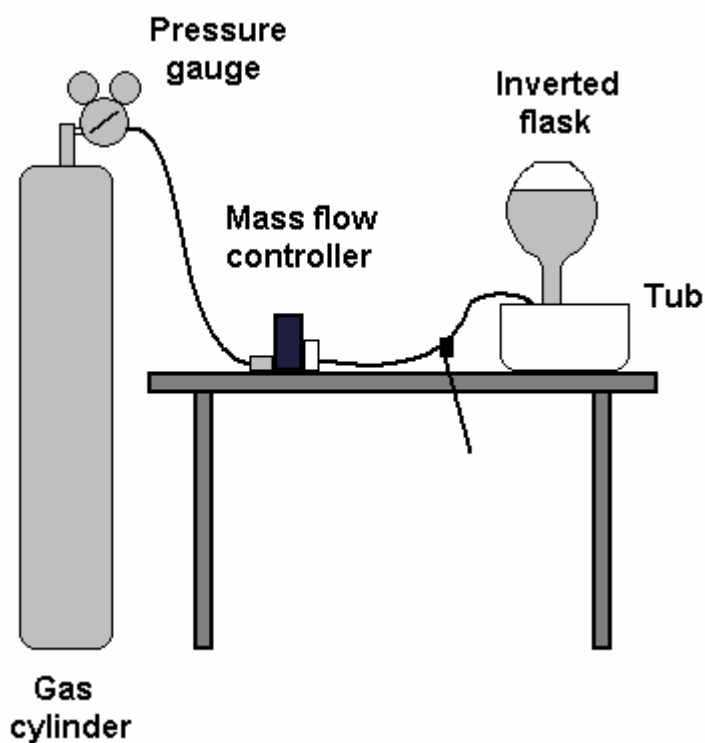
Figure 54. Calibration system of the mass flow controllers.

A flask was completely filled with water and the top of the flask was covered securely. The flask was then overturned and secured by a holding device as shown in Figure 54. After set-

ting the MFC to a desired value, the gas was flown until it reached a steady state. After the steady state was reached, the tube with the gas flowing through it was placed at the bottom of the flask. The insertion of the tube into the flask and the starting of the stopwatch were done at the same time. While the gas was filling the flask, the output value of the MFC was recorded to compare with the set flow rate. Once a reasonable amount of gas got filled into the flask, the tube was taken out from the flask and the timer was stopped simultaneously. The height of the column of water in the flask was measured. The weight of the flask was taken.

From the data collected as above, the calibration file was prepared that produced a linear correlation between set value and actual value, where the slope of the trend line was nearly one.

APPENDIX 2

CATALYST SAMPLE DETAILS

The Cu-ZSM-5 catalyst sample was obtained from Johnson Matthey Technology Center, UK, upon contacting Mr. Stan Golunski, Research Leader, Automotive and Process Catalysis. Table 7 lists further details of the sample.

Table 7. Cu-ZSM-5 catalyst sample details.

Material	Ceramic honeycomb with square-cells
Cell density (cells/in^2)	413
Sample density (Kg/m^3)	605
Cu-loading, % (by weight)	5
Si:Al ratio	80:1
BET surface area (m^2/gm)	345
Operating temperature (advised)	300–550°C

The vanadium-based catalyst sample was obtained from Sud-Chemie Prototech Inc., USA, upon contacting Mr. Yinyan Huang, R&D Manager. Table 8 lists further details of the sample.

Table 8. Vanadium-based catalyst sample details.

Material	Cordierite ceramic honeycomb with square-cells
	Cordierite ceramic: 40–60 wt% Vanadium pentoxide (V$_2$O$_5$): <1 wt%
Cell density (cells/inch^2)	230
Sample density (Kg/m^3)	636
Geometric surface area / Geometric volume (cm^2/cm^3)	21.34
Operating temperature (advised)	< 500°C

APPENDIX 3

TEMPERATURE DISTRIBUTION IN THE FURNACE

A total of 1100 sccm of gas is flown through the Mass Flow Controllers. The furnace was turned on and set at elevated temperatures. It took a while for it to reach the steady state. The temperature distribution inside the furnace was taken at increments of 2 cm distance along the length using a K-type thermocouple. The results are shown in Figures 55–57.
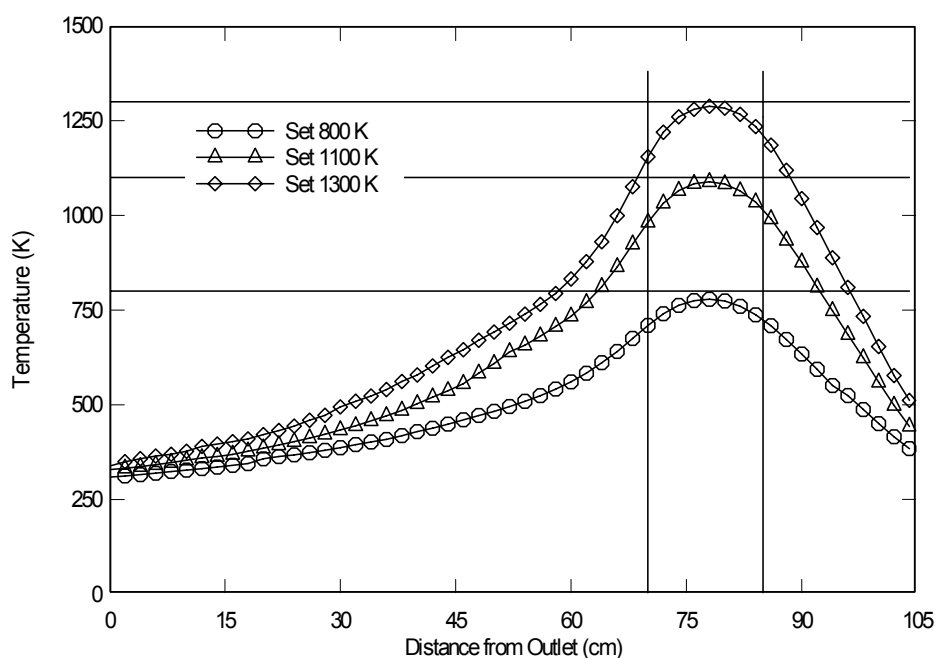

Figure 55. Axial temperature distribution with Zone-1 heated at 800, 1100 and 1300 K [32].

As can be observed from the figures, the temperature profile is not flat in the zone which is being heated. Towards both the ends of the zone, a temperature drop of up to 150 K occurs. This is true irrespective of the number of zones heated inside the reactor. The drop in temperature could be attributed to imperfect insulation, which leads to heat loss to the ambient atmosphere.
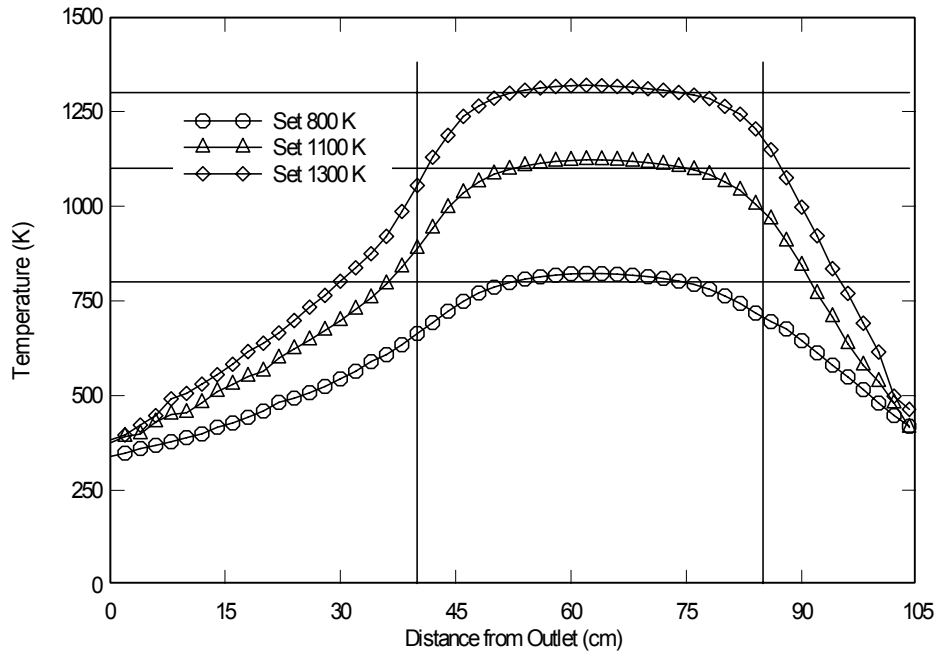
Figure 56. Axial temperature distribution with Zone-1 and Zone-2 heated at 800, 1100 and 1300 K [32].
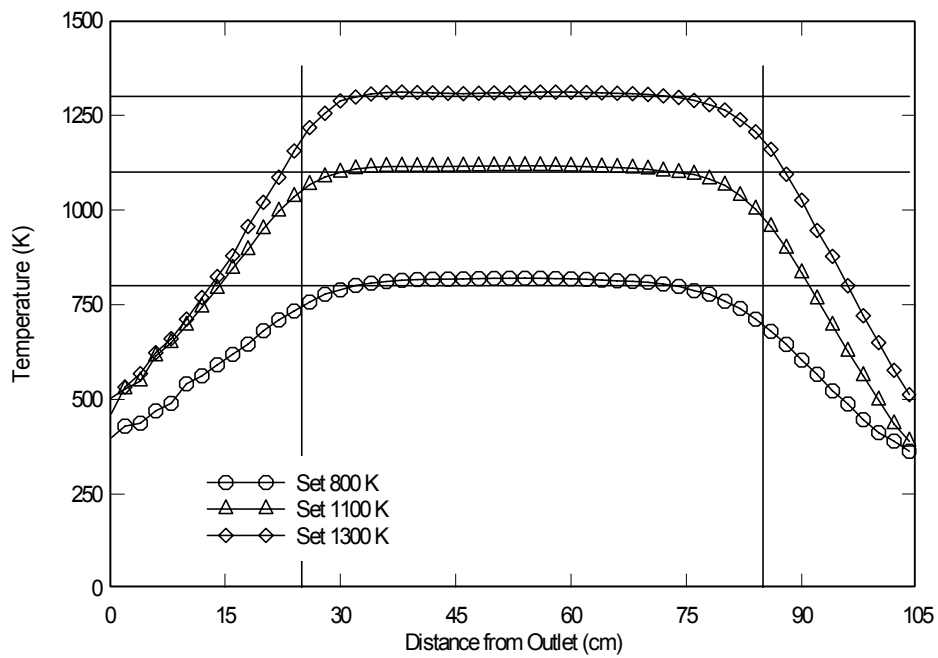

Figure 57. Axial temperature distribution with Zone-1, Zone-2, and Zone-3 heated at 800, 1100 and 1300 K [32].

VITA

Saurabh Gupta was born on May 2, 1978 in Rourkela, India. He enrolled in energy engineering at the Indian Institute of Technology (IIT), Kharagpur in the Fall of 1996 and received his Bachelor of Technology (Honors) degree in the Summer of 2000. He served as a Software Application Developer at Covansys (India) Private Limited, Chennai in 2000 and 2001. He enrolled at Texas A&M University in the Fall of 2001 to pursue a Master of Science in mechanical engineering.

Saurabh Gupta can be reached at: saurabh_kgp@yahoo.com. His permanent address is: B-167, Sector-20, Rourkela, India 769005.